NASA TN D-255

TECHNICAL NOTE

D-255

REQUIREMENTS OF TRAJECTORY CORRECTIVE IMPULSES DURING THE APPROACH PHASE OF AN INTERPLANETARY MISSION

By Alan L. Friedlander and David P. Harry, III

Lewis Research Center
Cleveland, Ohio

NATIONAL AERONAUTICS AND SPACE ADMINISTRATION

WASHINGTON

January 1960

NATIONAL AERONAUTICS AND SPACE ADMINISTRATION

TECHNICAL NOTE D-255

REQUIREMENTS OF TRAJECTORY CORRECTIVE IMPULSES DURING THE APPROACH PHASE OF AN INTERPLANETARY MISSION

By Alan L. Friedlander and David P. Harry, III

SUMMARY

The basic equations describing trajectory motion in the vicinity of a target body are presented in dimensionless form. The expressions are limited to two-dimensional orbital motion that is relative to a spherical planet influenced only by an inverse-square central force field. Corrective maneuvers executed during the approach phase of an interplanetary flight are studied. Optimization techniques are used to determine the minimum velocity impulse required to correct initial perigee errors, the numerical solution being obtained iteratively with the aid of a digital computer. The magnitude and alinement of the minimum impulse vector are presented for an extensive range of initial conditions. It is found that the related cost requirement, in terms of impulse magnitude, increases with the time necessary to detect and correct "off-course" trajectories. The minimum corrective impulses associated with the approach phase are compared with the total requirements of a round-trip Mars mission.

Impulsive thrusts applied in directions other than optimum are analyzed to determine deviations from the minimum magnitudes. Circumferential impulses, which can be calculated from an algebraic expression, offer an excellent approximation under certain initial conditions; namely, if the correction is executed at a radial distance much greater than the target perigee. Expressions for the errors in corrected perigee (miss distance) due to magnitude and directional errors of the applied velocity impulse are presented for the case of circumferential thrust. An example of a trajectory utilizing atmospheric deceleration demonstrates the critical effect of cutoff errors and gives some measure of the accuracy required in the control of the velocity vector.

INTRODUCTION

When considering interplanetary flights, it is recognized that simple ballistic trajectories will meet with little success. A study by

Ehricke (ref. 1) shows that the accuracy requirements during the initial launch phase appear technically unfeasible. Therefore, it is reasonable to expect a space probe will be equipped with a navigation and guidance system that will allow trajectory corrections en route.

The main goal of both the launch and midcourse guidance phase is to assure a successful rendezvous with the heliocentric orbit of the destination planet at the proper time and place. Upon arriving at the destination, the velocity of the space vehicle will, in general, differ from the orbital velocity of the target planet. This difference is called the hyperbolic velocity relative to the planet (ref. 2). The attracting body causes the vehicle to move along a hyperbolic approach trajectory. Because of various perturbations, such as guidance errors, the initial trajectory will most likely differ from the desired one. It will therefore be necessary to correct the trajectory. A convenient measure of the significant trajectory parameters is the perigee (distance of closest approach).

The major objective of this report is to present an analysis of the minimum velocity impulse required to correct perigee errors. The target perigee is chosen based upon mission requirements such as the establishment of a satellite orbit or possibly the use of atmospheric deceleration. However, in order not to limit the results, the solution will be considered independent of the maneuver executed upon reaching the target perigee. A study is also made of velocity impulses alined in directions other than the optimum to determine the penalties in energy expenditure due to departure from optimum.

In support of the necessity of perigee corrections, two methods of transferring from an approach trajectory to a circular satellite orbit are investigated and compared on the basis of velocity requirements. The total velocity impulses associated with interplanetary flights are presented in reference 2 for an idealized trajectory assuming no path corrections upon approaching the target planet. The results of the present study may be used to calculate the contribution of corrective impulses to overall mission requirements. Also included in this report is an analysis illustrating the effects of impulse alinement and magnitude errors upon the corrected trajectory. The accuracy required in the control of the impulse vector may be estimated if the permissible error in the target perigee is given.

The results of this report are not intended to apply to an actual space flight. The fundamental relations describing trajectory motion are limited to the assumption of a two-body, two-dimensional problem. Since the scope of the analysis is defined only in the vicinity of the target planet, this assumption is felt to be valid. The results and conclusions should be useful to any future comprehensive mission analysis.

SYMBOLS

A	dimensionless semimajor axis, a/r_{p_2}
a	semimajor axis, miles
E	dimensionless total energy per unit mass, $2\mathscr{E}/(v^*_{p_2})^2$
$\mathscr{E}$	total energy per unit mass, $(\text{miles/sec})^2$
G	universal gravitational constant
H	dimensionless angular momentum per unit mass, $h/v^*_{p_2} r_{p_2}$
h	angular momentum per unit mass, $\text{miles}^2/\text{sec}$
M	mass of planet
R	dimensionless radial distance (range), r/r_{p_2}
R_p	dimensionless perigee of trajectory, r_p/r_{p_2}
r	radial distance measured from center of planet (range), miles
r_p	perigee of trajectory, miles
V	dimensionless velocity, $v/v^*_{p_2}$
ΔV	dimensionless velocity impulse, $\Delta v/v^*_{p_2}$
v	velocity, miles/sec
v^*_p	velocity of escape at perigee, miles/sec
α	trajectory angle, angle between local horizontal and trajectory tangent, deg
β	velocity impulse angle with respect to initial velocity vector, deg

Subscripts:

c	circular
e	escape

h	hyperbolic
i	entry
min	minimum
opt	optimum
t	total
t.e.	transfer ellipse
I	first impulse
II	second impulse
1	conditions of initial approach trajectory
2	conditions of desired approach trajectory

ANALYSIS

Method of Analysis

Assumptions. - In order to simplify the following analysis, certain assumptions and approximations are made. Trajectory motion during the approach phase is considered to be relative to the attractive body and influenced only by an inverse-square central force field. Furthermore, the mass of the vehicle is insignificant in comparison to that of the attracting body. Only high-thrust devices are considered. The velocity impulses are therefore associated with negligible burning times relative to trajectory time scales, and the direction of the velocity impulse vector can be considered constant. Also, the corrective impulses are applied in a constant plane of motion. Initial trajectory parameters, such as velocity, perigee, and radial distance, are accurately known. Therefore, trajectory corrections can be made at a reasonably large distance from the planet.

In an actual flight situation many of these assumptions may not be valid. For instance, perturbing effects of moons, unsymmetrical gravitational fields, instrument errors, and three-dimensional motion must be taken into account. The results of this report are intended only to define the nature of corrective maneuvers and to aid in the rapid estimation of velocity requirements.

Normalized trajectory equations. - If the results of this analysis are to be applicable to any target planet, the basic equations describing

trajectory motion must be transformed to a dimensionless, or normalized, form. This is achieved by using the perigee of the desired approach trajectory and the escape velocity at this radial distance as the normalizing factors. In this way the target perigee remains a variable and yet is eliminated as a separate system parameter.

The normalization procedure is applied to the two basic equations describing motion along the trajectory, namely the conservation of both energy and angular momentum. Since the classical two-body problem has been assumed, the total energy per unit mass is given by the sum of kinetic and potential energy:

$$\mathscr{E} = \frac{v^2}{2} - \frac{GM}{r} \tag{1}$$

The angular momentum per unit mass is

$$h = vr \cos \alpha \tag{2}$$

where α (see fig. 1) is the trajectory angle between the velocity vector and the perpendicular to the radial vector. The velocity of escape is defined as the velocity along a parabolic orbit ($\mathscr{E} = 0$). Therefore, at the perigee of a desired approach path the velocity of escape is a constant given by

$$(v^*_{p_2})^2 = \frac{2GM}{r_{p_2}} \tag{3}$$

The defining equations of the normalization are

$$\left.\begin{aligned} V &= \frac{v}{v^*_{p_2}} \\ R &= \frac{r}{r_{p_2}} \\ E &= \frac{2\mathscr{E}}{(v^*_{p_2})^2} \\ H &= \frac{h}{v^*_{p_2} r_{p_2}} \end{aligned}\right\} \tag{4}$$

Equations (1) and (2) may now be divided by $(v^*_{p_2})^2$ and $v^*_{p_2} r_{p_2}$, respectively, and rewritten in dimensionless form:

$$E = V^2 - \frac{1}{R} \tag{5}$$

$$H = VR \cos \alpha \tag{6}$$

The trajectory angle at the perigee of any approach path is identically zero. Since equations (5) and (6) are conservative, they may be combined for conditions at the perigee. The angular momentum is thus shown to be a function of energy and perigee:

$$H^2 = R_p^2 E + R_p \tag{7}$$

The trajectory angle is now given as

$$\cos \alpha = \sqrt{\frac{R_p^2 E + R_p}{R^2 E + R}} \tag{8}$$

Range of initial conditions. - A summary of planetary data presented in references 2 and 3 is listed in table I. All quantities in the table are either given in dimensional units or are referred to conditions at the surface of the planet.

Row 3 represents a good estimate of the maximum radial distance (range) where a space probe could be considered influenced mainly by the force field of the attracting body. Values of initial perigee both greater and less than the target perigee will be investigated. The initial energy of an approach trajectory is equal to the square of the normalized hyperbolic velocity. The values given in rows 4 and 5 must first be normalized to the target perigee. For the purpose of this analysis, a reasonable range of initial conditions is taken as

$$0.01 \leq R \leq 100$$

$$0.01 \leq R_{p_1} \leq 100$$

$$0 \leq E_1 \leq 1.0$$

It should be mentioned that negative energies (elliptical trajectories) may be of interest. The subsequent equations will be valid for this case; however, results will be discussed only in terms of higher energy trajectories.

Throughout the analysis all equations will be written in normalized form, and most results and conclusions will be discussed in terms of normalized parameters. This should not cause the reader to lose sight of the physical significance of the results. For a given problem the

desired conditions are fixed. Therefore, the dimensionless parameters are directly proportional to the real parameters.

Perigee Corrections - Minimization of Velocity Impulse

The gravitational field of an attracting body causes a space vehicle entering the field to move along an approach trajectory relative to the body. With reference to figure 1, assume that the perigee (distance of closest approach) of the initial trajectory differs from a desired or target perigee. The target perigee is chosen based on mission requirements such as the establishment of a satellite orbit, or possibly the use of atmospheric deceleration. A velocity impulse must therefore be applied to correct the initial perigee error. The impulse required can be minimized by orienting the thrust vector in the proper direction.

Characteristics of optimum solution. - From the trigonometric relations of figure 1,

$$\Delta V^2 = V_1^2 + V_2^2 - 2V_1V_2 \cos(\alpha_2 - \alpha_1) \tag{9}$$

and

$$\sin \beta = \frac{V_2 \sin(\alpha_2 - \alpha_1)}{\Delta V} \tag{10}$$

To perform the optimization, the total derivative of equation (9) is taken and equated to zero, all quantities with subscript 1 being constant:

$$V_2 - \frac{V_1}{V_2} \cos(\alpha_2 - \alpha_1)V_2 = - V_1V_2 \sin(\alpha_2 - \alpha_1) \frac{d\alpha_2}{dV_2} \tag{11}$$

From equations (5), (6), and (7), where $R_{p_2} = 1$ by definition,

$$E_2 = V_2^2 - \frac{1}{R} = H_2^2 - 1 = (V_2R \cos \alpha_2)^2 - 1$$

or

$$V_2^2 = \frac{R - 1}{R(R^2 \cos^2\alpha_2 - 1)} \tag{12}$$

This equation defines the general vector $\overline{V}_2$ that is required to satisfy the corrected trajectory.

Differentiating equation (12), R being constant,

$$V_2 = - V_2^2 \left(\frac{\cos \alpha_2 \sin \alpha_2}{\frac{1}{R^2} - \cos^2 \alpha_2} \right) \frac{d\alpha_2}{dV_2}$$

Substituting this result into equation (11) and simplifying give

$$\frac{V_2}{V_1} = \frac{\sin \alpha_1}{\sin \alpha_2} \left(1 - \frac{1}{R^2} \right) + \frac{1}{R^2} \frac{\cos \alpha_1}{\cos \alpha_2} \tag{13}$$

Equations (12) and (13) act together to define optimum conditions; however, any algebraic manipulation leads to a polynomial equation of such high degree that the task of extracting the real roots becomes impractical. Since high-speed computing facilities were avilable, it was considered expedient to obtain a trial-and-error iterative solution. This was accomplished as follows.

In equation (13), α_2 was used as the trial value based initially upon the knowledge of α_1; V_2 was obtained from equation (13) and then substituted into equation (12), thereby giving a new value of α_2 that was treated by a forced conversion technique. The looping terminated when successive values of V_2 agreed to six significant digits. The resulting values of $(V_2, \alpha_2)_{opt}$ were used in equations (9) and (10) to obtain the optimum (minimum) velocity impulse vector $(\Delta V, \beta)$.

Care was exercised in the iterative treatment to assure that the solution yielded the proper root corresponding to minimum conditions. To assist in explaining the characteristics of the optimum solution, consider equation (12). For a given initial trajectory and range R, V_2 is found corresponding to any choice of α_2. The velocity increment is then calculated from equation (9).

Figure 2(a), plotted for $E_1 = 0$, $R_{p_1} = 5$, and $R = 50$, shows the effect of the trajectory angle on the size of the corrective impulse. For this plot, α_2 is defined as the angle measured clockwise from the vector V_2 to the horizontal direction. For the purpose of explanation, the figure is divided into four quadrants. A vector V_2 lying in the first quadrant designates counterclockwise motion directed toward the attracting body. Similarily, second-, third-, and fourth-quadrant vectors designate clockwise-toward, clockwise-away, and counterclockwise-away motion, respectively. The latter two can be dismissed, since only motion that approaches the target body is of interest here. Furthermore, it can

be said intuitively that, unless rotational changes are warranted, impulses that act to maintain the initial rotation should be less costly. This is substantiated by the graph, which shows two distinct optimums, one occurring at $\alpha_2 = 81.53^\circ$ and the other at $\alpha_2 = 98.47^\circ$. The corresponding impulse magnitudes are 0.0247 and 0.0648, respectively, the former being the minimum solution. In this example there is a small band of trajectory angles ($88.85^\circ < \alpha_2 < 91.15^\circ$) that result in a nonreal impulse. It can be shown from equation (12) that this band increases with decreasing R.

To illustrate the sensitivity in the vicinity of the minimum, a magnified plot is shown in figure 2(b). Whereas the minimum impulse is highly sensitive to the trajectory angle, it is very insensitive to the thrust direction. For example, a ΔV change of 0.01 on both sides of the minimum corresponds to a 2.9° change in α_2 and an 86° change in β.

The optimum solution has been discussed for a particular set of initial conditions. Although numerical results and sensitivities will vary with initial conditions, the general characteristic of figure 2(a) can be anticipated. The iterative solution was employed to calculate a multitude of data points with no apparent discrepancy; therefore, the true minimum solution is assumed.

In the event that a corrective impulse is applied at the perigee of the approach trajectory, equation (13) is reducible and the optimization may be treated analytically. This special case is discussed in appendix A.

Characteristics of minimum velocity impulse. - The minimum impulse has been calculated for an extensive range of initial conditions and is illustrated in figure 3 for an arbitrary energy E_1 of 0.05.

The magnitude of ΔV is plotted in figure 3(a) as a function of initial perigee for a family of constant radial distance. An initial perigee R_{p_1} of 1 represents an initial "on-course" trajectory; therefore, ΔV is zero at this point. As the initial perigee deviates from unity, the required impulse increases. Also, for a given perigee, the greater the range at which the correction is made, the smaller the velocity impulse.

The optimum impulse angle β_{opt} is shown in figure 3(b). It is noted that β_{opt} approaches 90° as R_{p_1} approaches unity. Also, if the correction is made at a large distance from the planet, the optimum angle is quite insensitive to the initial perigee, but becomes increasingly

sensitive with decreasing R. Consequently, when R is small and $R_{p_1} > 1$, a significant error in the corrected perigee can be expected because of thrust misalinement. This result is demonstrated by a detailed error analysis later in this report.

A most interesting and useful result is

$$(\Delta V)_{R_{p_1},E_1} \approx \frac{1}{R} \tag{14}$$

The inverse proportionality is illustrated in figure 3(c), where the data presented in figure 3(a) are plotted as a function of R for a family of constant R_{p_1}. The log-log scale is chosen to demonstrate an approximate slope of -1. For a given trajectory the maximum deviation occurs when $R = R_{p_1}$. The accuracy of the approximation increases with decreasing perigee. For example, the maximum errors at $R_{p_1} = 5$ and 2 are about 5.4 and 32 percent, respectively. However, for most conditions the error is insignificant and expression (14) offers an excellent approximation. This result was found to apply equally well for all values of initial energy and perigee studied.

In general, the minimum impulse causes a change in the velocity and therefore a change in the energy of the approach trajectory. This effect is shown in figure 3(d). For a given R, the larger the required perigee correction, the larger the energy change. The most significant characteristic is that the energy is decreased if the initial perigee is greater than the target perigee and vice versa. The importance of this fact is realized when consideration is given to type of maneuver executed upon arriving at the target perigee. Assume the mission requirement calls for a satellite orbit around the planet, the energy of which is always less than the approach energy. Obviously, the less the difference between the two energies, the smaller will be the velocity increment needed to establish the satellite orbit. Therefore, if $R_{p_1} > 1$, the minimum impulse appears to have an added advantage in terms of the total mission.

Approximate calculation for general set of initial conditions. - Thus far, only the characteristics of the minimum impulse have been discussed. It would be useful to present the results in a manner that would enable one to obtain a rapid and reasonably accurate numerical answer for an arbitrary target planet and approach trajectory. This is accomplished using the approximation of equation (14). Figure 4, plotted for R = 50, shows the variation of minimum impulse with initial energy for a family of constant initial perigees. Therefore, given an arbitrary

set of initial conditions (E_1, R_{p_1}, R), ΔV_{min} is found by entering the graph with the particular E_1, interpolating for R_{p_1}, and multiplying the value of ΔV read off the ordinate scale by $50/R$.

As an example, consider approaching Venus along a hyperbolic trajectory described by the following parameters: $v_h = 1.70$ miles per second and $r_{p_1} = 4.95$ Venus radii. Furthermore, the initial perigee is to be corrected at a distance $r = 75$ Venus radii to a target perigee $r_{p_2} = 1.1$ Venus radii. The initial energy is the square of the hyperbolic velocity. Using the defining equations (4), the normalized parameters are found to be $E_1 = 0.075$, $R_{p_1} = 4.5$, and $R = 68.2$. From figure 4(a),

$$\Delta V \cong 0.03 \left(\frac{50}{68.2}\right) = 0.0222$$

Since the escape velocity at 1.1 radii is 6.2 miles per second = 32,750 feet per second, the minimum velocity impulse required is

$$\Delta v = (0.0222)(32,750) = 727 \text{ ft/sec}$$

Velocity Impulses Alined in Directions Other Than Optimum

For most initial conditions the corrective velocity impulse may be applied in any given direction, where the magnitude of the impulse is then dependent on direction. Heretofore, the case of the minimum impulse has been presented. There are at least three other well-defined directions in which a corrective impulse may be applied: tangential, radial, and circumferential. A fourth possibility is to apply thrust in such a direction that the energy remains the same before and after burning.

It would be of interest to study these cases individually in order to determine first, whether such corrections are feasible, and second, how and under what conditions they compare with the minimum. It would be extremely useful to obtain a simple algebraic expression that would closely approximate the minimum impulse. The analysis is presented in appendix B; the results are given herein.

Tangential impulse. - The velocity impulse for the tangential direction is

$$\Delta V = \left| \sqrt{E_1 + 1/R} - \sqrt{\frac{(E_1 R + 1)(R - 1)}{E_1 R^2 (R_{p_1}^2 - 1) + R(RR_{p_1} - 1)}} \right| \qquad (15)$$

Radial impulse. - The radial velocity impulse is

$$\Delta V = \frac{1}{R}\left|\sqrt{E_1 R_{p_1}^2 (R^2 - 1) + R^2(R_{p_1} - 1) + (R - R_{p_1})} - \sqrt{E_1(R^2 - R_{p_1}^2) + (R - R_{p_1})}\right| \quad (16)$$

Circumferential impulse. - The equation for circumferential impulse is

$$\Delta V = \frac{1}{R}\left|\sqrt{E_1 R_{p_1}^2 + R_{p_1}} - \sqrt{\frac{E_1(R^2 - R_{p_1}^2) + (R^2 - R_{p_1})}{R^2 - 1}}\right| \quad (17)$$

Zero-energy-change impulse. - The equation for no energy change is as follows:

$$\Delta V = 2\sqrt{E_1 + 1/R}\,\sin\left|\frac{1}{2}\cos^{-1}\sqrt{\frac{E_1 + 1}{R^2 E_1 + R}} - \frac{1}{2}\cos^{-1}\sqrt{\frac{R_{p_1}^2 E_1 + R_{p_1}}{R^2 E_1 + R}}\right| \quad (18)$$

Comparison with minimum impulse. - The required impulsive velocities corresponding to tangential, radial, circumferential, and zero-energy-change vectoring are given by equations (15), (16), (17), and (18), respectively. The first two are compared with ΔV_{min} and plotted in figure 5 for $E_1 = 0$ and $R = 100$. Tangential thrust approaches the minimum only when the initial perigee is equivalent to the range at which the thrust is applied. For all other conditions the deviation is considerable, the increase in ΔV being as much as 100-fold for small initial perigees. The use of radial thrust requires much larger ΔV values. In fact, for this example, radial thrust cannot be applied if $R_{p_1} < 0.99$ (see thrust limitations in appendix B). This deviation from the minimum has been found to be characteristic for all initial conditions (E_1, R_{p_1}, R) studied. It is concluded that corrective impulses alined in either the tangential or the radial direction are much too costly in terms of required velocity increment.

The velocity requirements of circumferential and zero-energy-change impulses are compared with the minimum in the following table:

R	$(\Delta V \times 10^2)_{min}$	$\Delta V \times 10^2$ ($\Delta E = 0$)	% deviation from min.	$\Delta V \times 10^2$ (circumferential)	% deviation from min.
$E_1 = 0, R_{p_1} = 10$					
100	2.163	2.211	2.2	2.163	0.00
50	4.328	4.531	4.7	4.328	.00
20	10.87	12.36	14.0	10.87	.00
10	22.09	36.98	67.0	22.09	0
$E_1 = 0, R_{p_1} = 1.175$					
4.90	1.763	1.890	7.2	1.805	2.4
2.94	3.159	3.620	14	3.285	4.0
2.45	3.992	4.580	14	4.185	4.8
1.96	5.523	6.230	13	5.890	6.7
1.47	9.648	11.21	16	11.48	19.0
1.175	29.17	36.40	25	29.80	2.2

The upper part of the table is for a parabolic approach trajectory having an initial perigee ten times as great as the target perigee. Zero-energy-change impulses are reasonably good approximations to the minimum when R is considerably larger than R_{p_1}. The maximum deviation occurs when the correction is made at the perigee. Circumferential impulses do not differ significantly from the minimum.

The second part of the table shows the effect when corrective thrust is applied near the target perigee. In the case of zero-energy-change impulses, the deviation increases as the range is decreased, and the order of magnitude is not unlike that of the first example. For circumferential impulses, the deviation is small when R is large, increases with decreasing R, and then becomes small again as $R \to R_{p_1}$. As discussed in appendix A, if thrust is applied at the perigee, the minimum velocity increment corresponds to circumferential alinement in most cases. If the approach trajectory is parabolic, this is true provided $R = R_{p_1} > 1.220$.

As a means of explaining the close equivalence of circumferential and minimum impulses, consider equation (13), which is the equation of condition for the optimization:

$$\frac{V_2}{V_1} = \frac{\sin \alpha_1}{\sin \alpha_2}\left(1 - \frac{1}{R^2}\right) + \frac{1}{R^2}\frac{\cos \alpha_1}{\cos \alpha_2} \qquad (13)$$

Now if R is much greater than the target perigee,

$$\frac{1}{R^2} \ll 1$$

and

$$\frac{\cos \alpha_1}{\cos \alpha_2} \ll R^2$$

then

$$\frac{V_2}{V_1} \cong \frac{\cos \alpha_1}{\sin \alpha_2}$$

But the relation that describes circumferential thrust is given by equation (B11):

$$\frac{V_2}{V_1} = \frac{\sin \alpha_1}{\sin \alpha_2}$$

Therefore, when the approximation is valid the minimum solution will yield a circumferential thrust. The magnitudes of the two terms in equation (13) are compared in the following table to illustrate the degree of approximation involved. The initial conditions chosen are identical to those in the preceding table, which compared the ΔV required for the minimum and circumferential impulses:

R	$\frac{\sin \alpha_1}{\sin \alpha_2}\left(1 - \frac{1}{R^2}\right)$	$\frac{1}{R^2}\frac{\cos \alpha_1}{\cos \alpha_2}$
$E_1 = 0$, $R_{p_1} = 10$		
100	0.953	0.000301
50	.905	.00115
20	.740	.00595
$E_1 = 0$, $R_{p_1} = 1.175$		
4.90	0.937	0.0445
2.94	.850	.123
2.45	.792	.177
1.96	.685	.277
1.47	.445	.492

The usefulness of equation (17) in estimating the minimum impulse is apparent in terms of reduced computing effort.

Transfer Maneuvers and Total Mission Requirements

Throughout the previous analysis the problem of correcting off-course approach trajectories to pass through a desired perigee has been investigated. The solution was considered independent of the type of maneuver executed upon reaching the perigee. In this section the method of perigee corrections is presented for a mission profile calling for more than a grazing pass or for the employment of atmospheric deceleration. Consideration is given to the case of establishing a circular satellite orbit at some specified altitude. Two methods of transferring from an approach trajectory to the satellite orbit are compared on the basis of velocity requirements.

Perigee intersection maneuver. - The perigee intersection maneuver involves two velocity impulses as shown in figure 1, one to correct the perigee of the initial approach trajectory to a perigee corresponding to the specified satellite radius, and the second to achieve circular velocity at this radius. The first impulse is based on the minimization technique previously discussed. The expression for the second is developed in appendix C:

$$\Delta V_t = \Delta V_I + \Delta V_{II} = \Delta V_{min} + \left(\sqrt{E_2 + 1} - \frac{1}{\sqrt{2}}\right) \tag{19}$$

It is recalled that E_2 is dependent upon ΔV_{min}.

Transfer ellipse maneuver. - The transfer ellipse maneuver (fig. 6(a)) requires no correction of the initial approach trajectory, provided it is not a collision course. Upon arriving at the perigee, a transition is made to a transfer ellipse that is tangent to both the initial trajectory and the satellite orbit. A second velocity impulse at the latter point of tangency establishes circular velocity. The total velocity requirement is derived in appendix C:

$$\Delta V_t = \sqrt{E_1 + \frac{1}{R_{p_1}}} - \frac{1}{\sqrt{R_{p_1}(R_{p_1} + 1)}} + \left|\sqrt{\frac{R_{p_1}}{R_{p_1} + 1}} - \frac{1}{\sqrt{2}}\right| \tag{20}$$

The absolute-value signs are necessary to include either initial condition, $R_{p_1} > 1$ or $R_{p_1} < 1$.

Comparison of transfer maneuvers. - The two methods of transfer maneuver are compared on the basis of total velocity requirements. Equations (19) and (20) are plotted in figure 7(a) for a parabolic approach trajectory ($E_1 = 0$). The minimum ΔV_t (0.2929) is identical for both methods and corresponds to an initial on-course trajectory.

When the initial perigee is greater than the target ($R_{p_1} > 1$), the velocity requirement of the transfer ellipse method reaches a maximum at about $R_{p_1} = 7$. The value of R_{p_1} at which this maximum occurs increases as the initial energy level is raised. The perigee intersection maneuver results in a sizable saving of velocity impulse over the transfer ellipse method. For example, if $R = 100$, a maximum reduction of about 35 percent occurs at $R_{p_1} = 7$.

Considering $R_{p_1} < 1$, it is seen that the perigee intersection maneuver requires a smaller total velocity impulse over the range of R studied. However, this characteristic is not generally true for all initial conditions.

A further comparison of the two transfer maneuvers is shown in figure 7(b), where the velocity is plotted as a function of the initial energy. The curves representing the transfer maneuvers correspond to a constant initial perigee of 0.1. The curve representing the initial on-course approach trajectory is calculated from equation (20), where $R_{p_1} = 1$. This curve intersects the transfer ellipse curve at $E_1 = 1$. In fact, it is possible to prove from equation (20) that an intersection always occurs at this point if $R_{p_1} < 1$. Therefore, if the initial conditions are such that the energy and perigee are greater and less than unity, respectively, it is surprisingly found that being off-course, in the proper direction, is an advantage.

Returning to the comparison, two curves representing the perigee intersection maneuver are shown. If the perigee correction is made at $R = 5$, this method requires less velocity impulse if $E_1 < 0.22$. Similarly, if $R = 10$, the energy need be less than 0.57. It is interesting to note that the characteristic for $R \to \infty$ coincides with the on-course curve. Consequently, this method is always more costly than the transfer ellipse maneuver for the conditions $R_{p_1} < 1$ and $E_1 > 1$.

Figure 7(c) shows the variation of velocity impulse with initial energy for a constant initial perigee of 10. Unlike figure 7(b), the perigee intersection maneuver appears always to require less ΔV.

The more efficient of the two transfer maneuvers thus depends upon the initial approach trajectory. If the initial perigee distribution were defined, the probability of one method requiring less velocity impulse than the other could be calculated for a specific mission. Although no attempt is made in this report to define such error distributions, based on the characteristics of figures 7 it is reasonably assumed that the method involving perigee corrections is the preferred one under most initial conditions.

Contribution of corrective impulses to total mission requirements. - Consider a round-trip Mars mission involving the transfer from a circular satellite orbit at 1.1 Earth radii to a similar orbit at 1.1 Mars radii. Assume the transfer orbit to be a minimum-energy, heliocentric ellipse. The hyperbolic velocities given in rows 4 and 5 of table I are here referred to the velocity of escape at 1.1 planet radii:

$$(E_1)_{Mars} = (V_h^2)_{Mars} = 1.1(0.512)^2 = 0.2880$$

$$(E_1)_{Earth} = (V_h^2)_{Earth} = 1.1(0.266)^2 = 0.0777$$

Assume perigee corrections are made far from the planet. For this example, $R = 50$ or $r = (50)(1.1) = 55$ planet radii.

The required velocity impulse corresponding to initial perigee errors can be found from figure 4(a). The escape velocities at 1.1 Mars and Earth radii, respectively, are calculated from row 2 of table I:

$$(v_e)_{Mars} = 3.22\sqrt{\frac{1}{1.1}} = 3.07 \text{ miles/sec} = 16.27\times10^3 \text{ ft/sec}$$

$$(v_e)_{Earth} = 6.95\sqrt{\frac{1}{1.1}} = 6.64 \text{ miles/sec} = 35.1\times10^3 \text{ ft/sec}$$

$R_{p_1} = \frac{r_{p_1}}{1.1}$	Δv, ft/sec	
	Mars	Earth
1.2	44	74
2	212	340
5	748	1122
10	1627	2250
20	3375	4270

The total mission requirement less corrective impulses has been calculated in reference 2:

$$\Delta v_t = 36{,}900 \text{ ft/sec}$$

For the purpose of this example, equal initial perigee errors are chosen upon arrival at both Mars and Earth. The contribution of corrective impulses to the total requirement is given by the following table:

$R_{p_1} = \frac{r_{p_1}}{1.1}$	$\Delta v_{Mars} + \Delta v_{Earth}$, ft/sec	Percent of total Δv
1.2	118	0.32
2	552	1.5
5	1870	4.8
10	3877	9.5
20	7645	17.0

The preceding results are presented to show the order of magnitudes involved in the correction of off-course trajectories. If the initial perigee distribution were defined, the corresponding thrust distribution could be analyzed to yield a more complete and meaningful result. Such an analysis, however, would depend upon the details of initial launching errors, midcourse guidance, and perturbations en route, which are beyond the scope of this report.

Effects of Cutoff Errors

It would be of interest to define the "miss distance" resulting from errors in the application of the corrective thrust, thus giving some measure of the accuracy required in the control of the velocity vector. An error will be considered a small deviation of the velocity vector (in magnitude and/or direction) from the correct value, where the directional error is limited to the orbital plane. The analysis is based on the definition of total derivative and simple partial differentiating. Thus,

$$dR_{p_2} = \frac{\partial R_{p_2}}{\partial(\Delta V)}\, d(\Delta V) + \frac{\partial R_{p_2}}{\partial \beta}\, d\beta \tag{21}$$

Beginning with the relation $H_2^2 = R_{p_2}^2 E_2 + R_{p_2}$ and differentiating with respect to a variable y,

$$2H_2 \frac{\partial H_2}{\partial y} = 2R_{p_2} E_2 \frac{\partial R_{p_2}}{\partial y} + R_{p_2}^2 \frac{\partial E_2}{\partial y} + \frac{\partial R_{p_2}}{\partial y}$$

Since $R_{p_2} = 1$ at the point to be evaluated,

$$\frac{\partial R_{p_2}}{\partial y} = \frac{2H_2 \frac{\partial H_2}{\partial y} - \frac{\partial E_2}{\partial y}}{2E_2 + 1} \tag{22}$$

Now $H_2 = V_2 R \cos \alpha_2$, where R is constant:

$$\frac{\partial H_2}{\partial y} = R \cos \alpha_2 \frac{\partial V_2}{\partial y} - V_2 R \sin \alpha_2 \frac{\partial \alpha_2}{\partial y} \tag{23}$$

Also, $E_2 = V_2^2 - 1/R$, and

$$\frac{\partial E_2}{\partial y} = 2V_2 \frac{\partial V_2}{\partial y} \tag{24}$$

Substitution of (24) and (25) into (23) gives

$$\frac{\partial R_{p_2}}{\partial y} = \frac{2(H_2 R \cos \alpha_2 - V_2) \frac{\partial V_2}{\partial y} - 2H_2 V_2 R \sin \alpha_2 \frac{\partial \alpha_2}{\partial y}}{2E_2 + 1} \tag{25}$$

The variable y may refer either to ΔV or β. The evaluation of $\partial V_2/\partial y$ and $\partial \alpha_2/\partial y$ can be simplified by considering circumferential impulsive thrusts, which have previously been shown to approximate the minimum correction. This was carried out with reference to the trigonometric relations corresponding to figure 1, keeping in mind the two possible initial conditions $R_{p_1} \lesseqgtr 1$. The partial differentiation proceeded in general terms, keeping the identity of trajectory parameters E_2, V_2, H_2, and so forth, and only thereafter was evaluated at the circumferential condition. The results are given:

$$\frac{\partial R_{p_2}}{\partial(\Delta V)} = \pm \frac{2(R^2-1)^2 \sqrt{E_1(R^2 - R_{p_1}^2) + (R^2 - R_{p_1})}}{R\sqrt{R^2-1}\left[2E_1(R^2 - R_{p_1}^2) + (R^2 - 2R_{p_1} + 1)\right]} \quad \begin{cases} - \text{ if } R_{p_1} > 1 \\ + \text{ if } R_{p_1} < 1 \end{cases} \tag{26}$$

$$\frac{\partial R_{p_2}}{\partial \beta} = \frac{-2(R^2-1)\sqrt{E_1(R^2-R_{p_1}^2)+(R-R_{p_1})}\left|\sqrt{E_1 R_{p_1}^2 + R_{p_1}} - \sqrt{\frac{E_1(R^2-R_{p_1}^2)+(R^2-R_{p_1})}{R^2-1}}\right|}{R^2\left[2E_1(R^2 - R_{p_1}^2) + (R^2 - 2R_{p_1} + 1)\right]} \tag{27}$$

For the sake of simplifying the discussion of these results, an example was worked out. The example was chosen to demonstrate the critical effect of cutoff errors. An initial parabolic approach path relative to Earth was selected, the target perigee being at 40 miles altitude in order to take advantage of atmospheric deceleration.

The miss distance due to an error in impulse magnitude is shown in figure 8(a) as a function of initial perigee and range. There is a significant region ($R_{p_1} < 0.4R$) over which the error coefficient $\partial r_{p_2}/\partial(\Delta V)$ is relatively independent of initial perigee. Considering a given trajectory, the miss distance decreases with the range at which the corrective impulse is applied, the variation being approximately linear over the flat characteristic. As might be expected, the price of using a smaller velocity increment is an increased sensitivity to deviations in the magnitude of the applied increment.

The miss distance due to thrust misalinement is plotted in figure 8(b). The error coefficient $\partial r_{p_2}/\partial\beta$ approaches zero for two distinct conditions: (1) if the initial trajectory is on-course, and (2) if thrust is applied at the perigee. Considering a given trajectory, the error is minimized by applying thrust at a large range R, a fact that is compatible with the minimization of the required corrective impulse.

Although a detailed analysis of the effects of miss distance caused by cutoff errors is not within the scope of this report, mention is made of how such effects could be determined. Assuming the desired target perigee is chosen based upon a permissible atmospheric entry angle, the first step is to calculate the actual entry angle corresponding to the miss distance. As an illustration, consider initial entry into Earth's atmosphere (assumed spherically symmetric) at an altitude of 50 miles. The entry angle is simply the trajectory angle and for a parabolic approach is given by $\cos \alpha_i = \sqrt{r_p/4050}$; surface radius is approximately 4000 miles. It is realized that thrust application alters the energy of the trajectory; however, it is assumed that the change is insignificant when R is large. The vehicle therefore enters the atmosphere along an essentially parabolic trajectory, thus making the preceding expression for the entry angle applicable.

For this example, consider a trajectory having the following initial conditions: $R_{p_1} = 5$, $R = 50$. From figures 8(a) and (b), the miss distance due to magnitude and alinement errors is -11.2 miles/(ft/sec) and -0.47 mile per degree, respectively. Figure 9 is plotted to show the effects of such errors on the atmospheric entry angle. The angle corresponding to an on-course trajectory ($R_{p_2} = 4040$ miles) is 2.86°.

Since the upper limit of the atmosphere is taken at 50 miles altitude, it is apparent that errors that result in nonentry ($\cos \alpha_i > 1$) cannot be permitted. Therefore, from figure 9, the magnitude error should be greater than -0.88 foot per second, and the alinement error should be greater than -21.3°.

To define the limitation of errors that result in too large an entry angle presents a fairly difficult problem. It is recognized that entering the atmosphere at too great an angle may be prohibitive to the vehicle design (intolerable g loads and heating rates). A detailed atmospheric reentry study has been made by Chapman (ref. 4), in which methods are available to obtain the solution of permissible entry angles.

CONCLUDING REMARKS

The analysis presented in this report has established the relations necessary to the investigation of corrective maneuvers during the approach phase of an interplanetary flight. Trajectory equations were transformed to a dimensionless form so as to be applicable to all planetary bodies. The results are useful within the limitation of two-dimensional trajectories that are relative to a spherical body and influenced only by an inverse-square central force field. Furthermore, corrective thrusts were assumed impulsive and alined in the plane of motion.

A study was made of the minimum velocity impulse that must be applied to correct initial perigee errors. The complexity of the expressions resulting from the optimization prompted a trial-and-error iterative solution. The magnitude and alinement of the minimum velocity vector were determined and their corresponding variation with initial trajectory parameters discussed. As a means of minimizing the propellant consumption, it is desirable to initiate a corrective maneuver at a large distance from the planet where the trajectory velocity is relatively small. The impulse magnitude was shown to be approximately inversely proportional to the distance at which the thrust is applied if the latter is considerably greater than the target perigee. This effect makes possible a rapid estimation of the required impulse for any set of initial conditions.

Corrective thrusts alined in directions other than optimum were investigated. The size of the velocity increments corresponding to circumferential impulses closely approximates the minimum requirements; if corrections are executed at distances much greater than the target perigee, the difference in ΔV is insignificant. Thus, it is possible to estimate the minimum velocity impulse from a relatively simple algebraic expression.

The cost of correcting off-course approach trajectories was compared to the total requirement of a simplified Earth-Mars round-trip mission. Large deviations from a desired trajectory result in sizable velocity increments, the anticipation of which will significantly influence initial takeoff weights and payload limitations.

The effect of cutoff errors on the final perigee was analyzed. Errors in the magnitude of the velocity impulse result in miss distances that decrease with the range at which the corrective impulse is applied. Conversely, the miss distance due to alinement errors is minimized by applying thrust far from the planet. In the case of atmospheric reentry, it was indicated that close control of the impulse vector is necessary to accomplish successful reentry.

Lewis Research Center
National Aeronautics and Space Administration
Cleveland, Ohio, October 9, 1959

E-484

APPENDIX A

OPTIMUM SOLUTION - SPECIAL CASE ($R = R_{p_1}$)

When a corrective velocity impulse is applied at the perigee of an approach trajectory, certain peculiarities of the optimum solution are found. This situation is treated as follows. Equation (13) is rewritten:

$$\frac{V_2}{V_1} \sin \alpha_2 = \sin \alpha_1 \left(1 - \frac{1}{R^2}\right) + \frac{1}{R^2} \frac{\cos \alpha_1 \sin \alpha_2}{\cos \alpha_2} \tag{13}$$

At the perigee, $\alpha_1 = 0^\circ$; therefore,

$$\frac{V_2}{V_1} \sin \alpha_2 = \frac{\sin \alpha_2}{R^2 \cos \alpha_2} \tag{A1}$$

From the text,

$$V_2^2 = \frac{R - 1}{R(R^2 \cos^2 \alpha_2 - 1)} \tag{12}$$

Equations (A1) and (12) define the optimum condition.

Solution A: $\alpha_2 = 0^\circ$

The equality of (A1) is satisfied if $\alpha_2 = 0^\circ$. Therefore, one solution of the optimum requires a circumferential impulse that causes the vehicle to achieve an elliptical trajectory, the perigee of which is tangent to the target perigee when $R_{p_1} > 1$. If $R_{p_1} < 1$, the apogee of the ellipse is tangent to the target perigee. The velocity impulse can be found from equations (12) and (5):

$$\Delta V = |V_1 - V_2| = \left| \sqrt{E_1 + 1/R} - \sqrt{\frac{1}{R(R + 1)}} \right| \tag{A2}$$

Solution B: $\alpha_2 \neq 0^\circ$

Equation (A1) can now be divided by $\sin \alpha_2$:

$$\frac{V_2}{V_1} = \frac{1}{R^2 \cos \alpha_2} \tag{A3}$$

Solving for $\cos^2\alpha_2$ from equations (12), (A3), and (5),

$$\cos^2\alpha_2 = \frac{E_1R + 1}{R^2(-R^3 + R^2 + E_1R + 1)} \tag{A4}$$

Since equation (A3) must result in a real physical solution,

$$0 \leq \frac{E_1R + 1}{R^2(-R^3 + R^2 + E_1R + 1)} \leq 1 \tag{A5}$$

It is recognized that the term $(E_1R + 1)$ is always positive because V_1 must be positive. The restrictions placed on solution B result from equation (A5) and may be found from the following:

$$R^3 - R^2 - E_1R - 1 = 0 \tag{A6}$$

$$R^5 - R^4 - E_1R^3 - R^2 + E_1R + 1 = 0 \tag{A7}$$

As an illustrative example, consider a parabolic trajectory $(E_1 = 0)$. Equations (A6) and (A7) reduce to

$$R^3 - R^2 - 1 = 0 \tag{A8}$$

and

$$R^5 - R^4 - R^2 + 1 = 0 \tag{A9}$$

Only real, positive roots need be considered. From Descartes' sign rule, one positive root of equation (A8) and two positive roots of equation (A9) can be expected. The solution of equation (A8) is obtained from the cubic formula, and that of (A9) by approximation. The results are

From (A8): $0 < R < 1.466$

From (A9): $1 < R < 1.220$

Since the two inequalities must be compatible,

$$1 < R < 1.220$$

Therefore, for any value of R not within these limits, the expression (A3) leads to a nonreal solution. Consequently, the first solution $(\alpha_2 = 0^\circ)$ is the only one and can be shown to result in the minimum ΔV.

When $r < 1.220$, the velocity impulse corresponding to solution B is found from equations (A3), (12), (9), and (5):

$$\Delta V^2 = E_1\left(1 - \frac{1}{R^2}\right) + \frac{1}{R}\left(2 - \frac{1}{R^2}\right) - 1 \tag{A10}$$

For $E_1 = 0$,

$$\Delta V^2 = \frac{1}{R}\left(2 - \frac{1}{R^2}\right) - 1 \tag{A11}$$

The characteristic of this special case is shown in figure 10. The approach trajectory is parabolic, and the velocity impulse is applied at the perigee. The curve plotted for $R = 1.4$ exemplifies a single optimum. The minimum requirement occurs when ΔV is alined in the circumferential direction. An example of two optimums is illustrated by the curve $R = 1.1$. The minimum ΔV ($\alpha_2 = 13.8^\circ$) results from solution B. For this condition, a circumferential impulse corresponds to a relative maximum and requires a ΔV about 13.5 percent above ΔV_{min}.

APPENDIX B

VELOCITY IMPULSES ALINED IN DIRECTIONS OTHER THAN OPTIMUM

Expressions are derived herein that give the magnitude of the corrective velocity vector for impulsive thrust alined in tangential, radial, and circumferential directions. Also, the velocity requirement corresponding to zero-energy-change ($\Delta E = 0$) impulses is presented. In this analysis, absolute-value symbols will be used to account for either initial condition $R_{p_1} > 1$ or $R_{p_1} < 1$.

Case A: Tangential Thrust

From sketch (a),

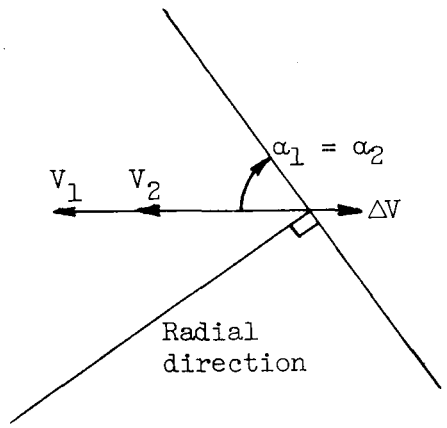

(a)

for tangential thrust,

$$\Delta V = |V_1 - V_2|$$

Since $\cos \alpha_1 = \cos \alpha_2$, the definition of angular momentum gives

$$\left(\frac{V_2}{V_1}\right)^2 = \left(\frac{H_2}{H_1}\right)^2 = \frac{E_2 + 1}{R_{p_1}^2 E_1 + R_{p_1}} = \frac{(V_2^2 - 1/R) + 1}{R_{p_1}^2 E_1 + R_{p_1}}$$

Solving for V_2^2 and simplifying, where $V_1^2 = E_1 + 1/R$,

$$V_2^2 = \frac{E_1 R(R - 1) + (R - 1)}{E_1 R^2(R_{p_1}^2 - 1) + R(RR_{p_1} - 1)}$$

Therefore,

$$\Delta V = \left| \sqrt{E_1 + 1/R} - \sqrt{\frac{(E_1 R + 1)(R - 1)}{E_1 R^2 (R_{p_1}^2 - 1) + R(RR_{p_1} - 1)}} \right| \tag{15}$$

Limitations on Use of Tangential Thrust

Under certain initial conditions the second radical of equation (15) may be negative, resulting in an imaginary solution. The term $(E_1 R + 1)$ is always positive:

$$\frac{R - 1}{E_1 R^2 (R_{p_1}^2 - 1) + R(RR_{p_1} - 1)} \geq 0 \tag{B1}$$

Considering values of R both greater and less than unity,

$$\left.\begin{aligned} R\left[E_1(R_{p_1}^2 - 1) + R_{p_1}\right] - 1 \geq 0 \qquad & \text{if} \quad R > 1 \\ R\left[E_1(R_{p_1}^2 - 1) + R_{p_1}\right] - 1 \leq 0 \qquad & \text{if} \quad R < 1 \end{aligned}\right\} \tag{B2}$$

For a given trajectory, expression (B2) defines the conditions under which a tangential thrust may be applied.

Case B: Radial Thrust

From sketch (b),

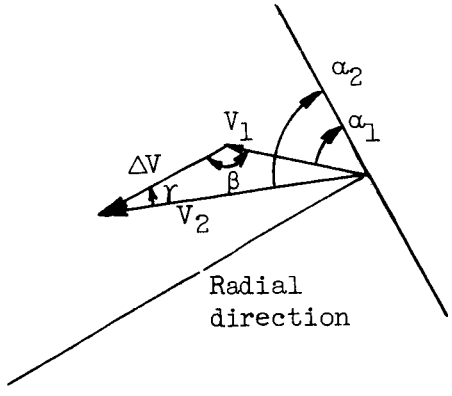

(b)

for radial thrust,

$$\beta = 90^\circ + \alpha_1$$

$$\gamma = 90^\circ - \alpha_2$$

From trigonometric relations,

$$\Delta V = |V_1 \cos \beta + V_2 \cos \gamma|$$

$$\Delta V = |V_2 \sin \alpha_2 - V_1 \sin \alpha_1| \qquad \text{(B3)}$$

Also,

$$V_2 = V_1 \frac{\sin \beta}{\sin \gamma} = V_1 \frac{\cos \alpha_1}{\cos \alpha_2} \qquad \text{(B4)}$$

Since $H = VR \cos \alpha$,

$$H_1 = H_2 \qquad \text{(B5)}$$

Substituting (B4) into (B3),

$$\Delta V = |V_1 \cos \alpha_1 \tan \alpha_2 - V_1 \sin \alpha_1| = V_1 \cos \alpha_1 |\tan \alpha_2 - \tan \alpha_1|$$

Therefore,

$$\Delta V = \frac{H_1}{R} |\tan \alpha_2 - \tan \alpha_1| \qquad \text{(B6)}$$

Since $H_1^2 = E_1 R_{p_1}^2 + R_{p_1}$ and $H_1^2 = H_2^2 = E_2 + 1$,

$$E_2 = R_{p_1}^2 E_1 + R_{p_1} - 1 \qquad \text{(B7)}$$

Now

$$\cos \alpha_1 = \frac{H_1}{V_1 R} = \frac{H_1}{R\sqrt{E_1 + 1/R}}$$

$$\cos \alpha_2 = \frac{H_1}{V_2 R} = \frac{H_1}{R\sqrt{E_2 + 1/R}} = \frac{H_1}{R\sqrt{E_1 R_{p_1}^2 + R_{p_1} - 1 + 1/R}}$$

Equation (B6) is now given in terms of initial conditions:

$$\Delta V = \frac{1}{R}\left|\sqrt{E_1 R_{p_1}^2 (R^2 - 1) + R^2(R_{p_1} - 1) + (R - R_{p_1})} - \sqrt{E_1(R^2 - R_{p_1}^2) + (R - R_{p_1})}\right| \tag{16}$$

Limitations on Use of Radial Thrust

As in case A, a limitation on the use of radial thrust presents itself. Consider the first radical of equation (16):

$$E_1 R_{p_1}^2 (R^2 - 1) + R^2(R_{p_1} - 1) + (R - R_{p_1}) \geq 0 \tag{B8}$$

Dividing by $(R - 1)$ and collecting terms,

$$R(E_1 R_{p_1}^2 + R_{p_1} - 1) + (E_1 R_{p_1}^2 + R_{p_1}) \geq 0 \tag{B9}$$

The second radical of equation (16) is $H_1 \tan \alpha_1$ and must be real. Therefore, the limitation on radial corrective impulses is given by the inequality (B9).

Case C: Circumferential Thrust

From sketch (c),

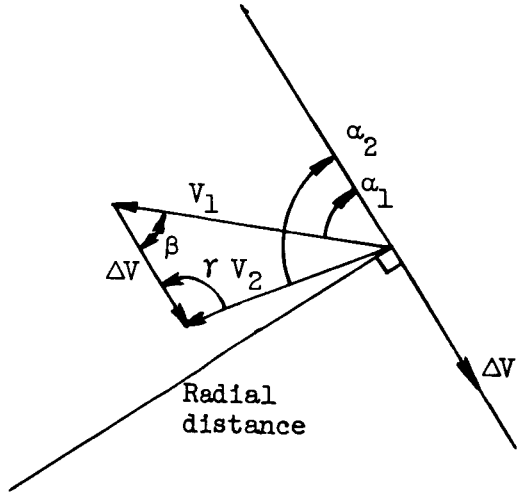

(c)

for circumferential thrust,

$$\beta = \alpha_1$$

$$\gamma = 180 - \alpha_2$$

$$\Delta V = |V_1 \cos \beta + V_2 \cos \gamma| = |V_1 \cos \alpha_1 - V_2 \cos \alpha_2|$$

$$\Delta V = \frac{1}{R}\left|V_1 R \cos \alpha_1 - V_2 R \cos \alpha_2\right|$$

Therefore,

$$\Delta V = \frac{1}{R}|H_1 - H_2| \tag{B10}$$

From the law of sines,

$$V_2 = V_1 \frac{\sin \beta}{\sin \gamma} = V_1 \frac{\sin \alpha_1}{\sin \alpha_2} \tag{B11}$$

Since $H_2^2 = (V_2 R \cos \alpha_2)^2 = E_2 + 1 = V_2^2 - 1/R + 1$,

$$V_2^2(R^2 \cos^2 \alpha_2 - 1) = \frac{R - 1}{R}$$

$$V_2^2(R^2 - R^2 \sin^2 \alpha_2 - 1) = \frac{R - 1}{R}$$

Substituting from (B11),

$$V_2^2(R^2 - 1) - V_1^2 R^2 \sin^2 \alpha_1 = \frac{R - 1}{R}$$

$$V_2^2 = E_2 + 1/R = \frac{\frac{R - 1}{R} + V_1^2 R^2 \sin^2 \alpha_1}{R^2 - 1}$$

Transposing, using $\cos^2 \alpha_1 = 1 - \sin^2 \alpha_1$, $V_1^2 = E_1 + 1/R$, $H = R_p^2 E + R_p$, and simplifying give

$$H_2^2 = E_2 + 1 = \frac{E_1(R^2 - R_{p_1}^2) + (R^2 - R_{p_1})}{R^2 - 1}$$

Equation (B10) may now be rewritten

$$\Delta V = \frac{1}{R}\left|\sqrt{E_1 R_{p_1}^2 + R_{p_1}} - \sqrt{\frac{E_1(R^2 - R_{p_1}^2) + (R^2 - R_{p_1})}{R^2 - 1}}\right| \qquad (17)$$

Limitations on Use of Circumferential Thrust

For limitations on the use of circumferential thrust, consider the second radical of equation (17). If a real solution is to be satisfied, then

$$\left.\begin{aligned} R^2(E_1 + 1) - (E_1 R_{p_1}^2 + R_{p_1}) &\geq 0 \qquad \text{if } R > 1 \\ R^2(E_1 + 1) - (E_1 R_{p_1}^2 + R_{p_1}) &\leq 0 \qquad \text{if } R < 1 \end{aligned}\right\} \qquad (B12)$$

Case D: Zero-Energy-Change Thrusts ($E_1 = E_2$)

From sketch (d),

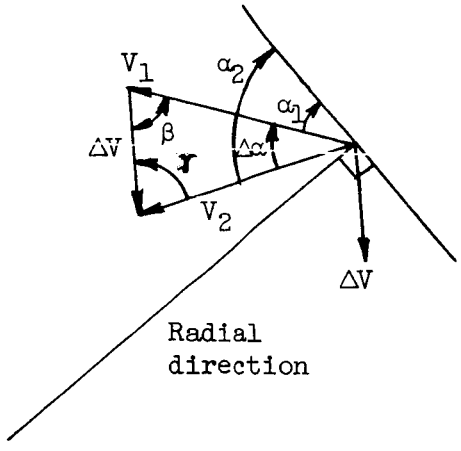

(d)

for zero-energy-change thrusts,

$$\gamma = \beta$$

$$V_2 = V_1$$

From the relations of an isosceles triangle,

$$\left.\begin{aligned} \Delta V &= 2V_1 \sin\left|\frac{\Delta\alpha}{2}\right| \\ \sin\beta &= \frac{\sin\Delta\alpha}{2\sin\frac{\Delta\alpha}{2}} \end{aligned}\right\} \qquad \text{(B13)}$$

From equations (5) and (8), where $R_{p_2} = 1$,

$$\Delta V = 2\sqrt{E_1 + 1/R}\,\sin\left|\frac{1}{2}\cos^{-1}\sqrt{\frac{E_1+1}{R^2E_1+R}} - \frac{1}{2}\cos^{-1}\sqrt{\frac{R_{p_1}^2E_1 + R_{p_1}}{R^2E_1+R}}\right| \qquad (18)$$

Limitation on Use of Zero-Energy-Change Thrusts

Since the cosine of an angle must be real and not greater than unity,

$$0 \le \frac{E_1+1}{R^2E_1+R} \le 1 \qquad \text{(B14)}$$

The solution of (B14) at the two limits results in the condition ($R > 1$, $E_1 > -1$). A corrective impulse of this type must be applied at a distance greater than the target perigee.

APPENDIX C

DEVELOPMENT OF EQUATIONS DESCRIBING TRANSFER MANEUVERS

Perigee Intersection Maneuver

The execution of the perigee intersection maneuver is illustrated in figure 1. The first velocity impulse (ΔV_I) acts to correct the initial perigee, and its magnitude is calculated based on the minimization analysis described earlier in the report. The second impulse is applied at the target perigee in a direction opposite to the vehicle velocity. The required circular velocity is simply

$$V_c = \sqrt{\frac{1}{2R_{p_2}}} = \frac{1}{\sqrt{2}}$$

since $R_{p_2} = 1$ by definition. The trajectory velocity at the perigee is, from equation (5),

$$\sqrt{E_2 + 1}$$

The second impulse is therefore

$$\Delta V_{II} = \sqrt{E_2 + 1} - \frac{1}{\sqrt{2}}$$

and the total requirement for the maneuver is

$$\Delta V_t = \Delta V_I + \Delta V_{II} = \Delta V_{min} + \left(\sqrt{E_2 + 1} - \frac{1}{\sqrt{2}}\right) \tag{19}$$

Transfer Ellipse Maneuver

The transfer ellipse maneuver is shown in figure 6(a):

$$\Delta V_t = \Delta V_I + \Delta V_{II} \tag{C1}$$

From the geometry of the figure, the semimajor axis is, by definition,

$$A_{t.e.} = \frac{R_{p_1} + R_{p_2}}{2} = \frac{R_{p_1} + 1}{2} \tag{C2}$$

The semimajor axis can also be related to the total energy of the elliptical transfer orbit (ref. 5):

$$A_{t.e.} = -\frac{1}{2E_{t.e.}} \tag{C3}$$

Therefore, from equations (C2) and (C3),

$$E_{t.e.} = -\frac{1}{R_{p_1} + 1} \tag{C4}$$

The required velocity along the ellipse at the initial perigee is

$$\sqrt{E_{t.e.} + \frac{1}{R_{p_1}}} = \frac{1}{\sqrt{R_{p_1}(R_{p_1} + 1)}} \tag{C5}$$

while the velocity along the approach path at R_{p_1} is

$$\sqrt{E_1 + \frac{1}{R_{p_1}}} \tag{C6}$$

The first retrothrust impulse is the difference between (C6) and (C5):

$$\Delta V_I = \sqrt{E_1 + \frac{1}{R_{p_1}}} - \frac{1}{\sqrt{R_{p_1}(R_{p_1} + 1)}} \tag{C7}$$

The two possible initial conditions for this maneuver are shown in figure 6. If $R_{p_1} > 1$, the second application of thrust is at the perigee of the transfer ellipse and directed opposite to the path velocity in order to achieve the lower value of circular velocity. If $R_{p_1} < 1$, thrust is applied at the apogee and colinear with the path velocity. In either case, the velocity at the point of tangency to the satellite orbit is, from the conservation of angular momentum,

$$\sqrt{\frac{R_{p_1}}{R_{p_1} + 1}} \tag{C8}$$

The second impulse is the absolute difference of (C8) and circular velocity. The absolute value is necessary to include either initial condition:

$$\Delta V_{II} = \left| \sqrt{\frac{R_{p_1}}{R_{p_1} + 1}} - \frac{1}{\sqrt{2}} \right| \tag{C9}$$

Equation (C1) now is given as

$$\Delta V_t = \sqrt{E_1 + \frac{1}{R_{p_1}}} - \frac{1}{\sqrt{R_{p_1}(R_{p_1} + 1)}} + \left| \sqrt{\frac{R_{p_1}}{R_{p_1} + 1}} - \frac{1}{\sqrt{2}} \right| \qquad (20)$$

REFERENCES

1. Ehricke, Krafft A.: Error Analysis of Keplerian Flights Involving a Single Central Force Field and Transfer Between Two Central Force Fields. Navigation, vol. 6., no. 1, 1958, pp. 5-23.

2. Moeckel, W. E.: Interplanetary Trajectories with Excess Energy. Paper presented at Int. Astronautical Cong., Amsterdam (Holland), Aug. 23-30, 1958.

3. Moeckel, W. E.: Trajectories with Constant Tangential Thrusts in Central Gravitational Fields. NASA TR R-53, 1959.

4. Chapman, Dean R.: An Approximate Analytical Method for Studying Entry into Planetary Atmospheres. NACA TN 4276, 1958.

5. Moulton, Forest Ray: An Introduction to Celestial Mechanics. Second Revised ed., The Macmillan Co., 1947.

TABLE I. - PLANETARY DATA

	Mercury	Venus	Earth	Mars	Jupiter	Saturn	Uranus	Neptune
1. Mean radius, miles	1550	3750	3960	2108	44,350	37,500	16,450	15,450
2. Surface escape velocity, miles/sec	1.99	6.51	6.95	3.22	38.04	23.53	14.40	12.95
3. Distance where solar gravitational effect is 10 percent planet's effect, planet radii	4.07	76.7	109	148	345	500	1220	2190
4. Hyperbolic velocity at Earth's orbit upon arrival from destination planet (escape velocities at surface of Earth)[a]	-0.224	-0.224	---	0.266	0.786	0.919	1.010	1.046
5. Hyperbolic velocity at destination orbit upon arrival from Earth (escape velocities at surface of planet)[a]	2.99	0.261	---	0.512	-0.092	0.143	0.203	0.194

[a]Calculated for minimum-energy heliocentric transfer orbits.

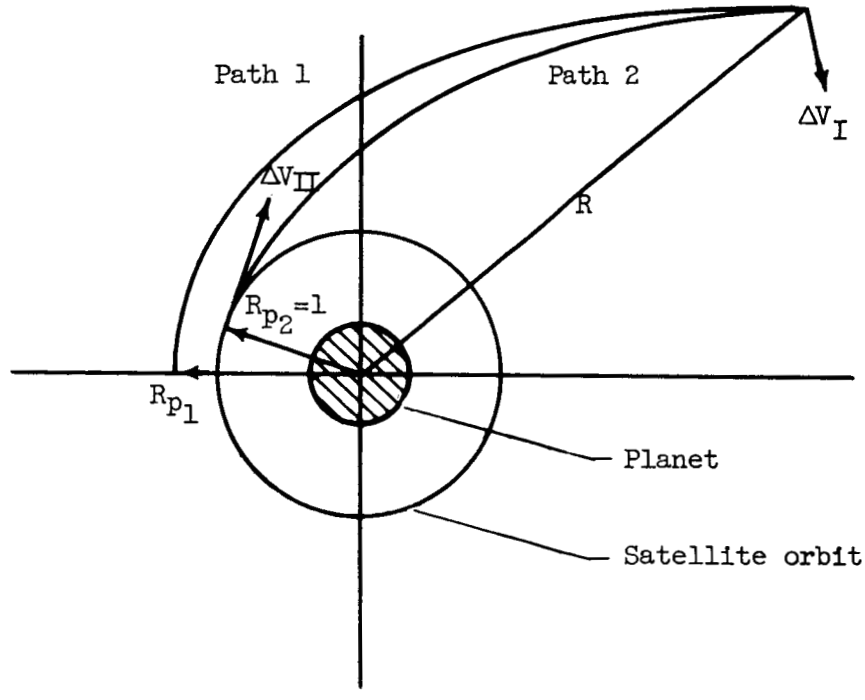

(a) Motion in orbital plane.

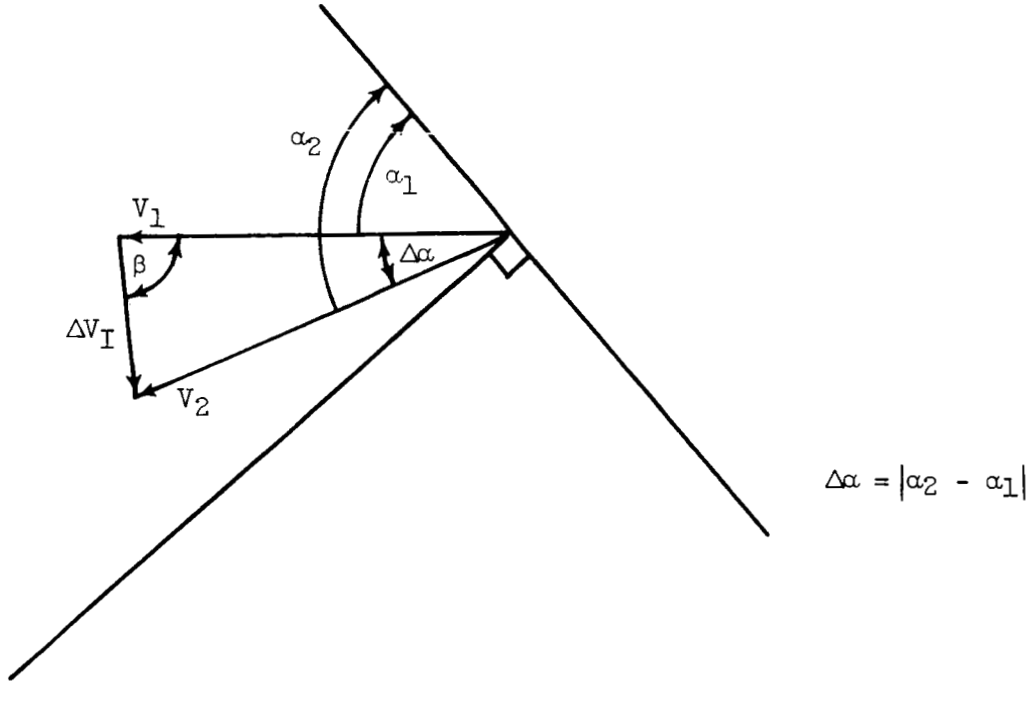

(b) Velocity correction diagram.

Figure 1. - Relative motion and velocity correction diagrams.

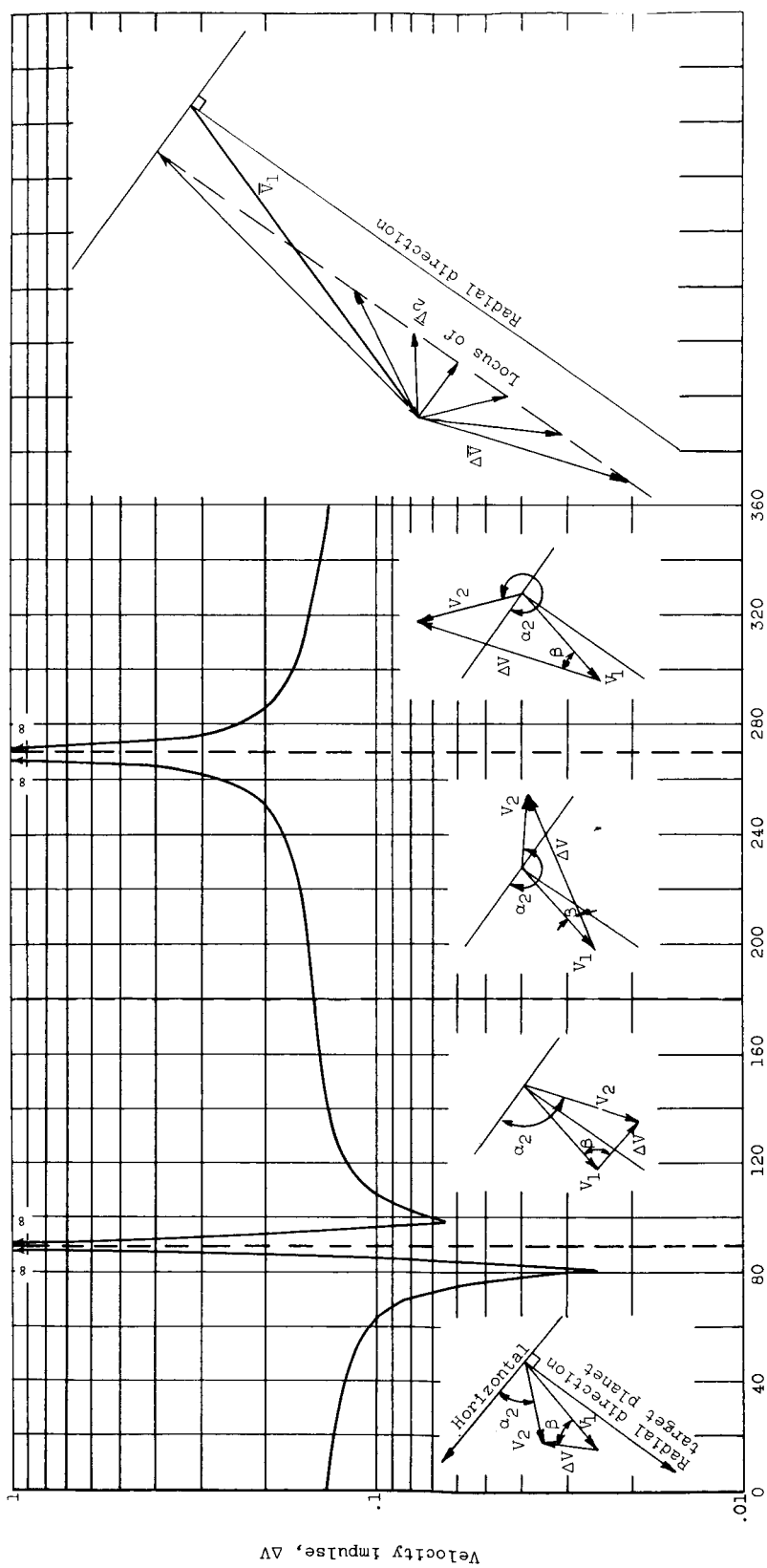

(a) Effect of trajectory angle on impulse magnitude. $E_1 = 0$; $R_{p_1} = 5$; $R = 50$.

Figure 2. - Corrective velocity impulse required to attain desired trajectory ($R_{p_2} = 1$).

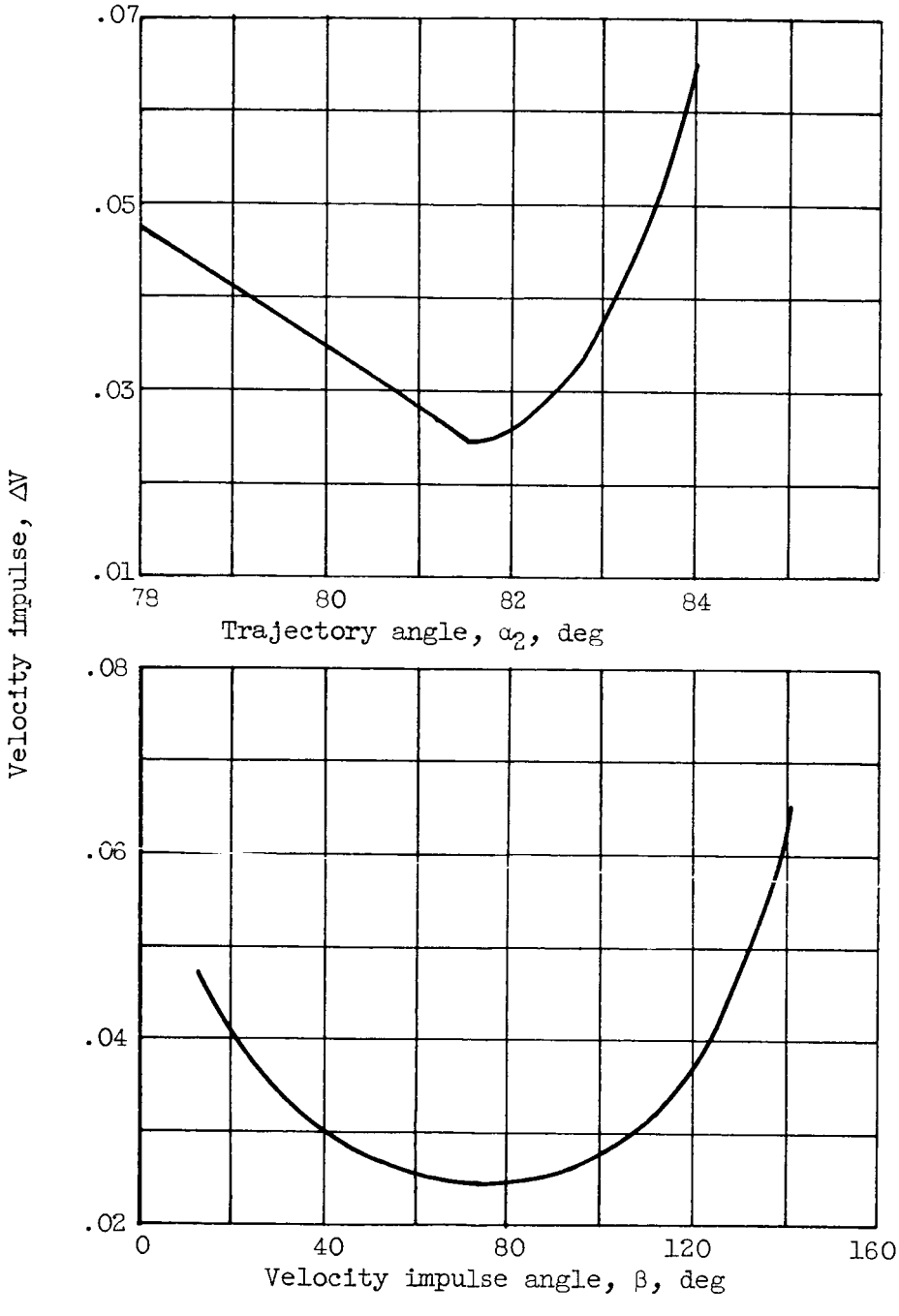

(b) Velocity impulse in vicinity of optimum.

Figure 2. - Concluded. Corrective velocity impulse required to attain desired trajectory ($R_{p_2} = 1$).

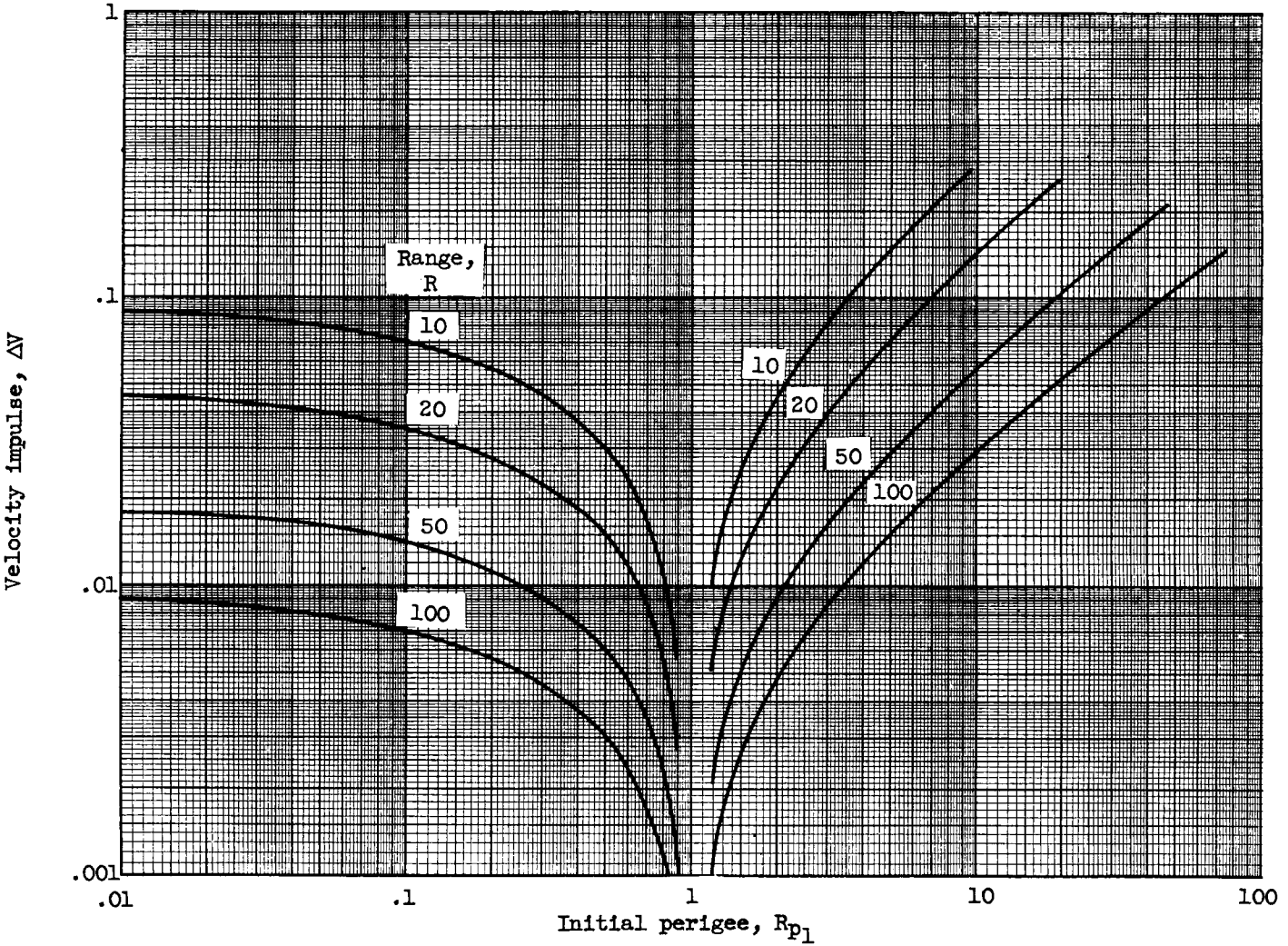

(a) Minimum velocity requirement of perigee corrections.

Figure 3. - Characteristics of minimum velocity impulse. Initial energy, E_1, 0.05.

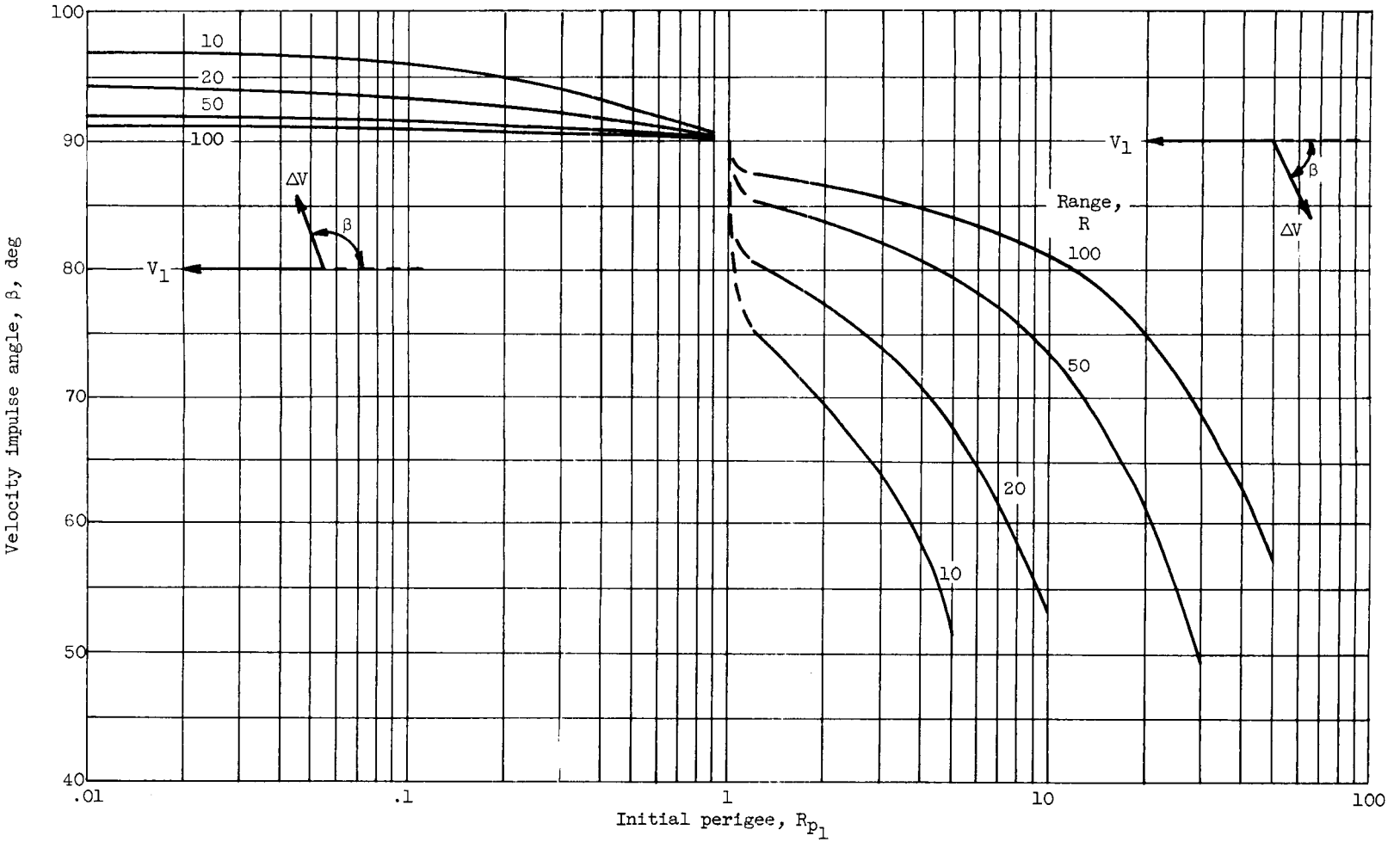

(b) Optimum velocity impulse angle.

Figure 3. - Continued. Characteristics of minimum velocity impulse. Initial energy, E_1, 0.05.

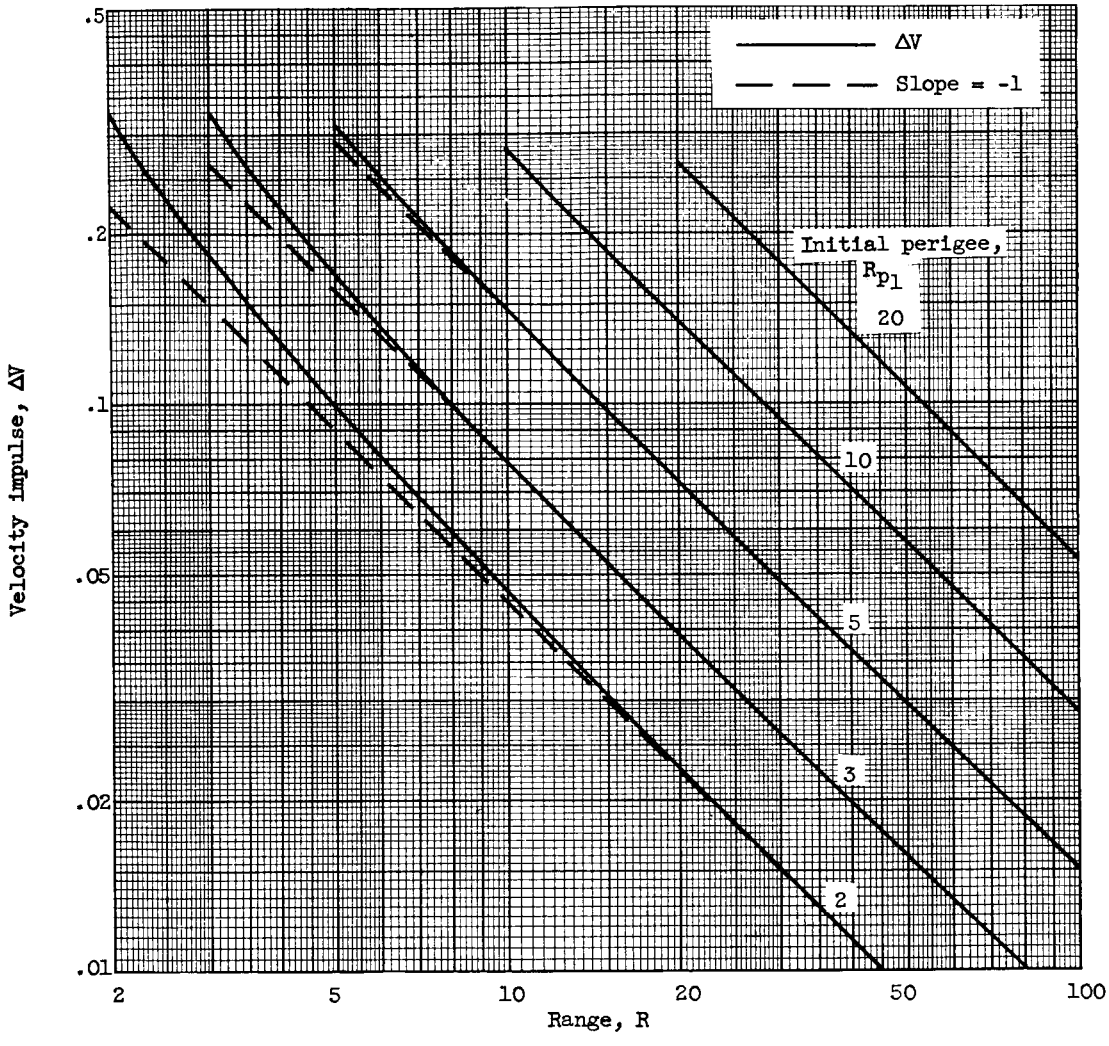

(c) Velocity impulse against range.

Figure 3. - Continued. Characteristics of minimum velocity impulse. Initial energy, E_1, 0.05.

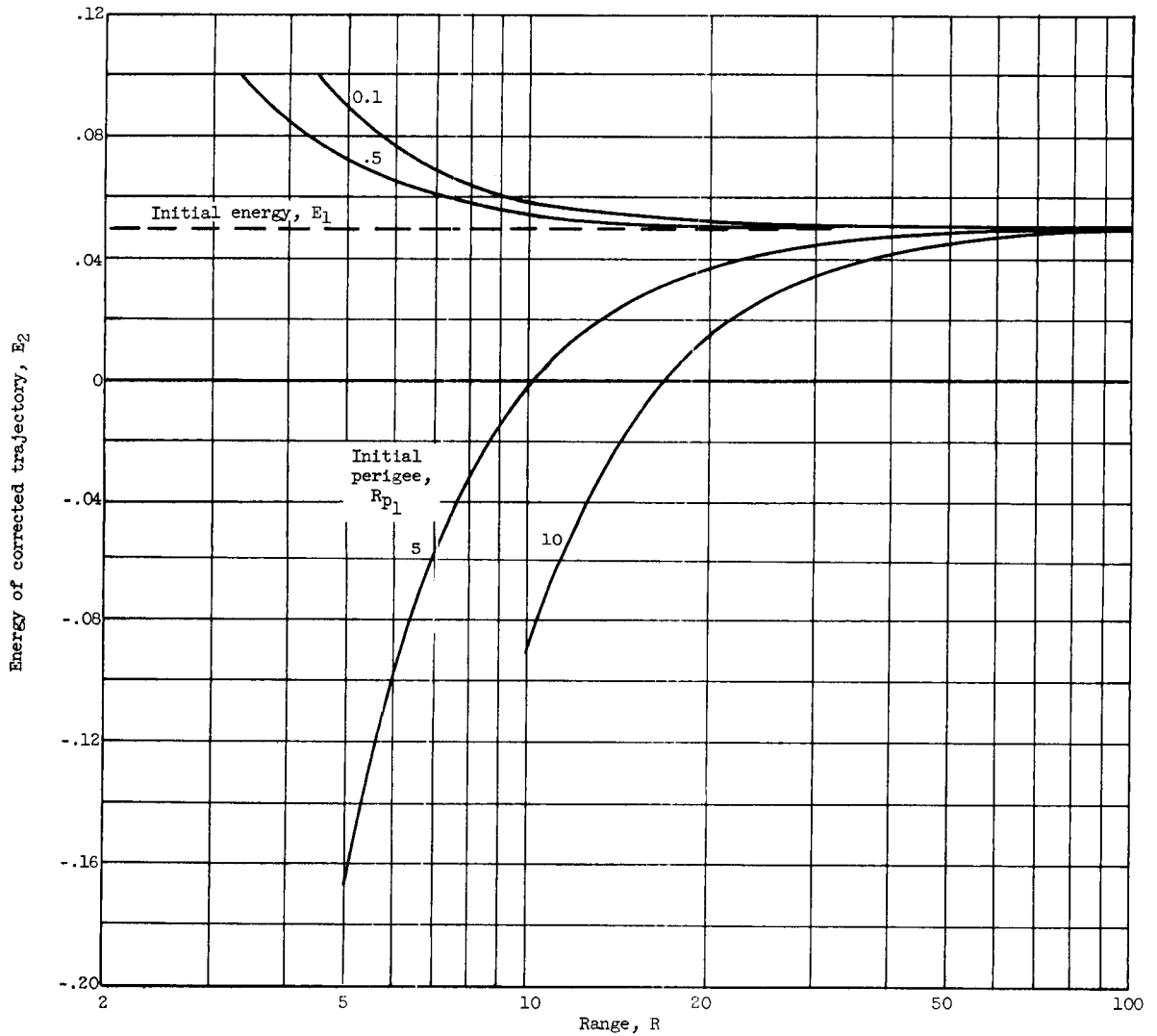

(d) Effect of minimum velocity impulse on energy level of trajectory.

Figure 3. - Concluded. Characteristics of minimum velocity impulse. Initial energy, E_1, 0.05.

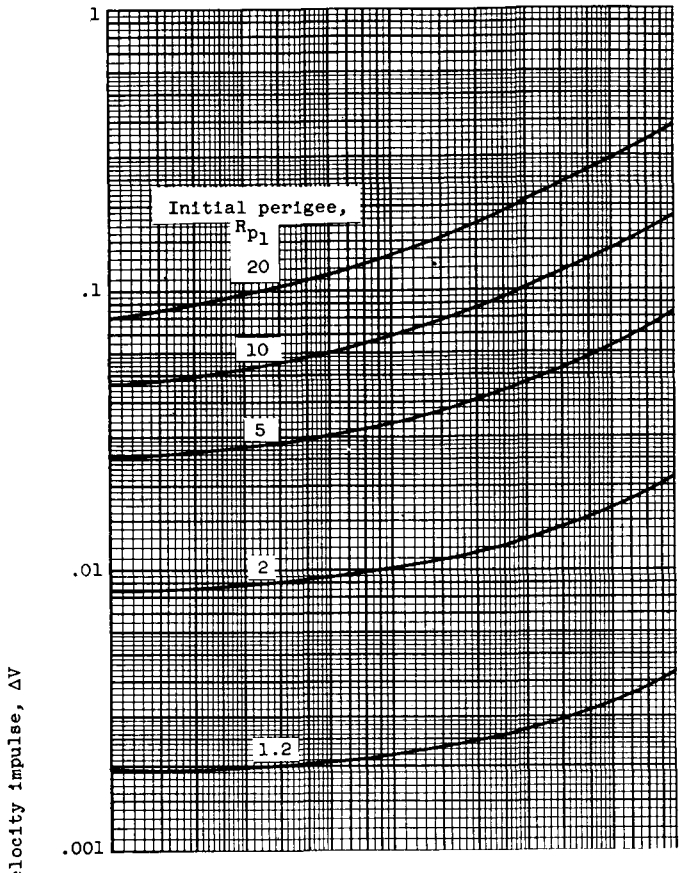

(a) Initial perigee, $R_{p_1} > 1$.

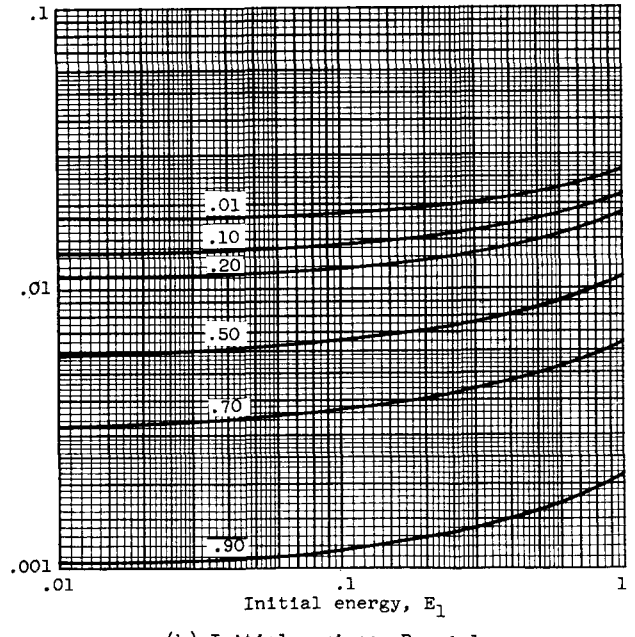

(b) Initial perigee, $R_{p_1} < 1$.

Figure 4. - Variation of velocity impulse with initial energy ratio. Optimum perigee corrections. Range, R, 50.

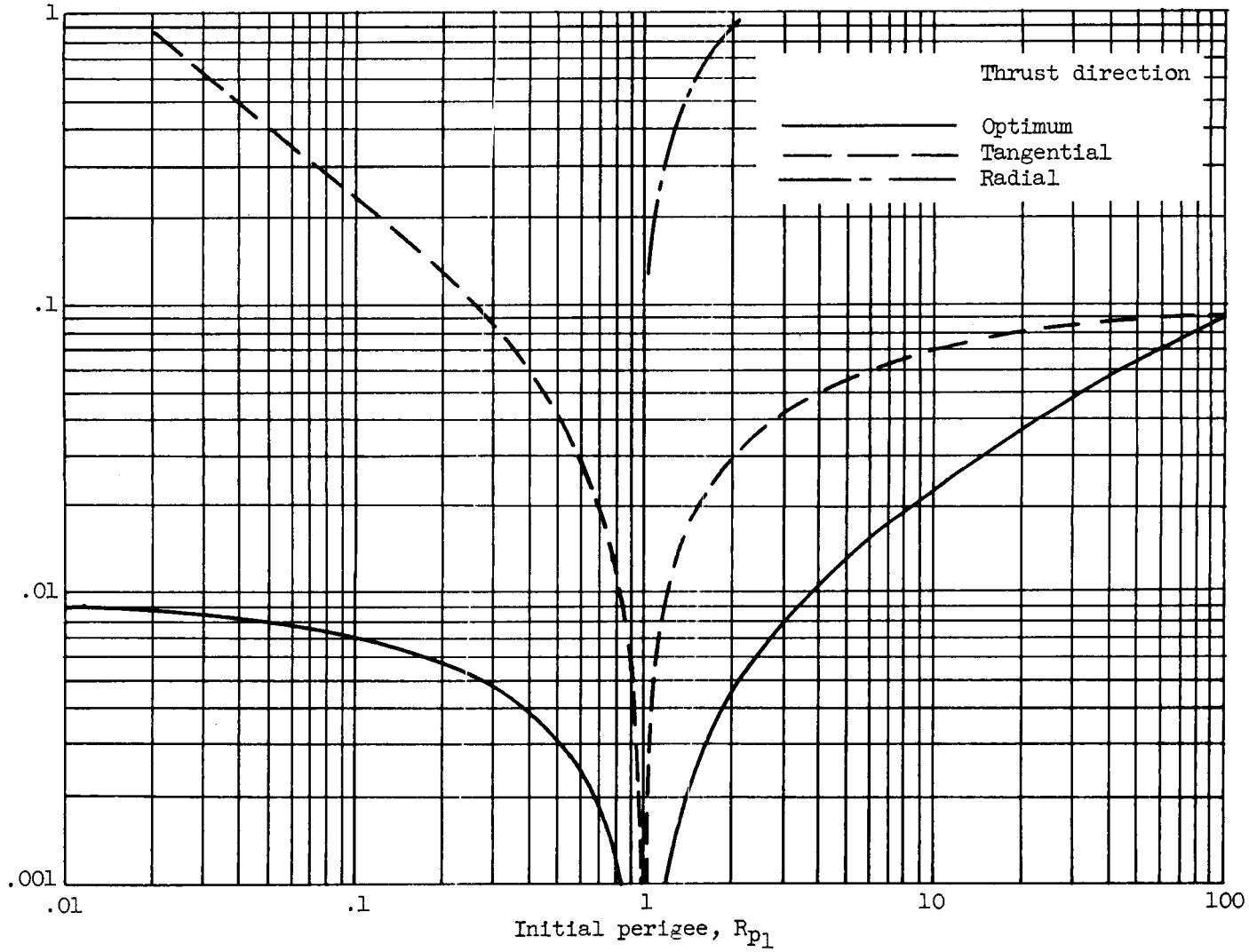

Figure 5. - Comparison of velocity impulses alined in optimum, tangential, and radial directions. Initial energy, E_1, 0; range, R, 100.

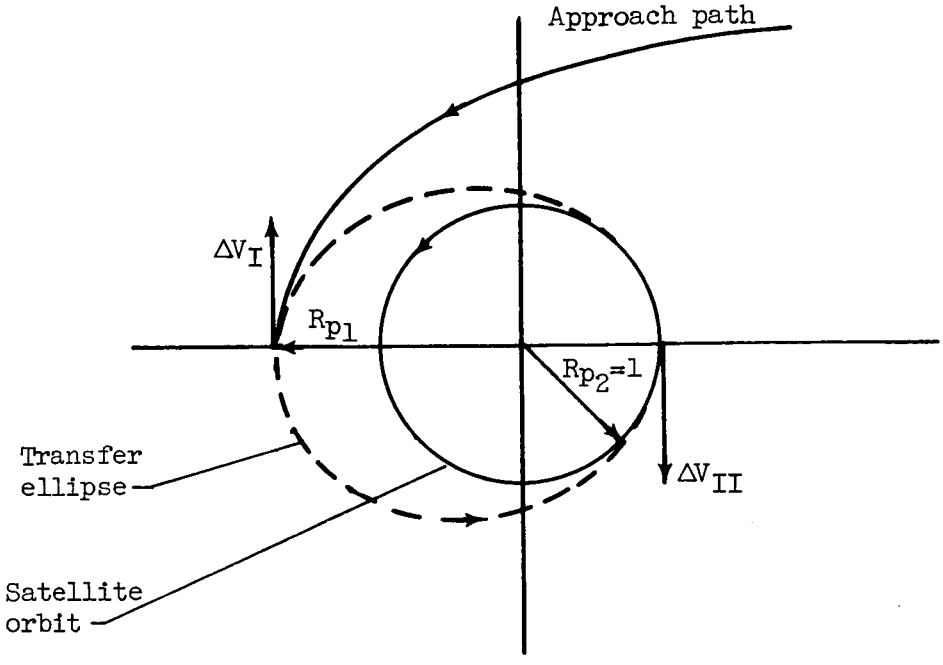

(a) $R_{p_1} > 1$.

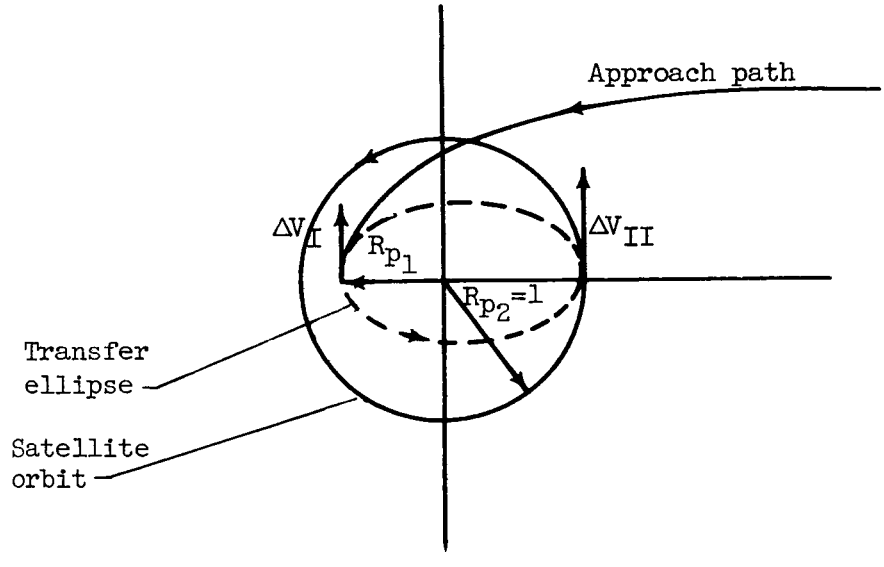

(b) $R_{p_1} < 1$.

Figure 6. - Transfer ellipse maneuver.

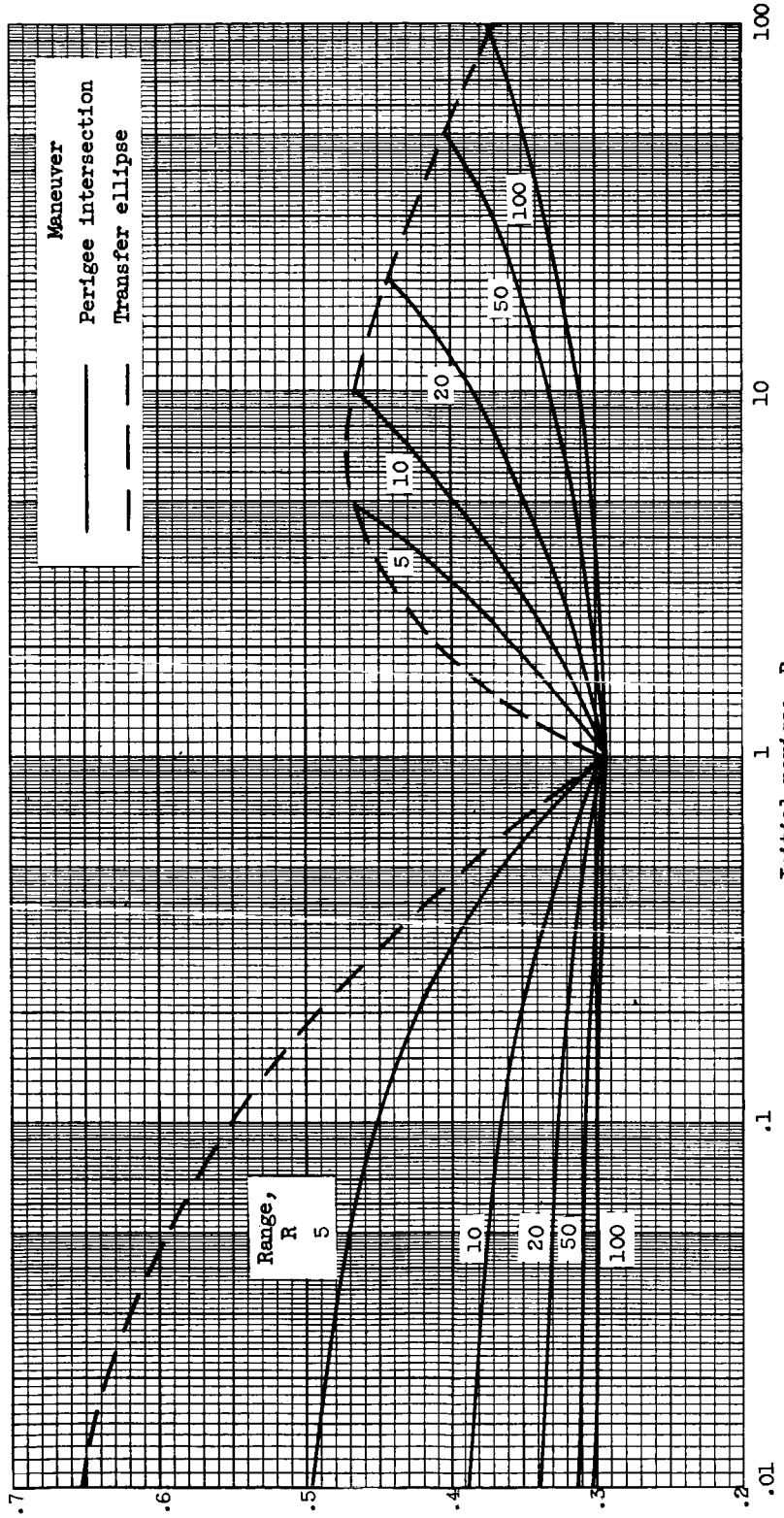

(a) Initial energy, E_1, 0.

Figure 7. - Required velocity impulse to transfer from approach trajectory to circular satellite orbit.

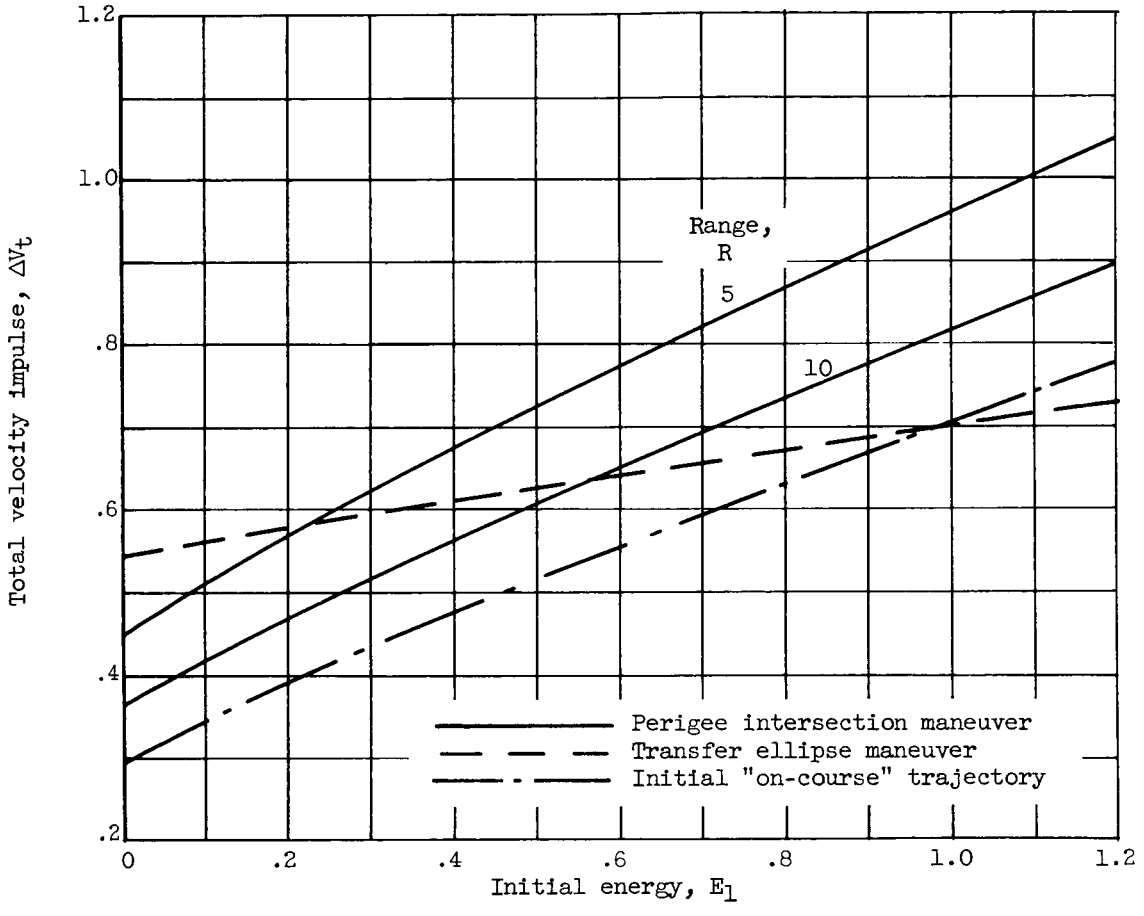

(b) Initial perigee, R_{p_1}, 0.1.

Figure 7. - Continued. Required velocity impulse to transfer from approach trajectory to circular satellite orbit.

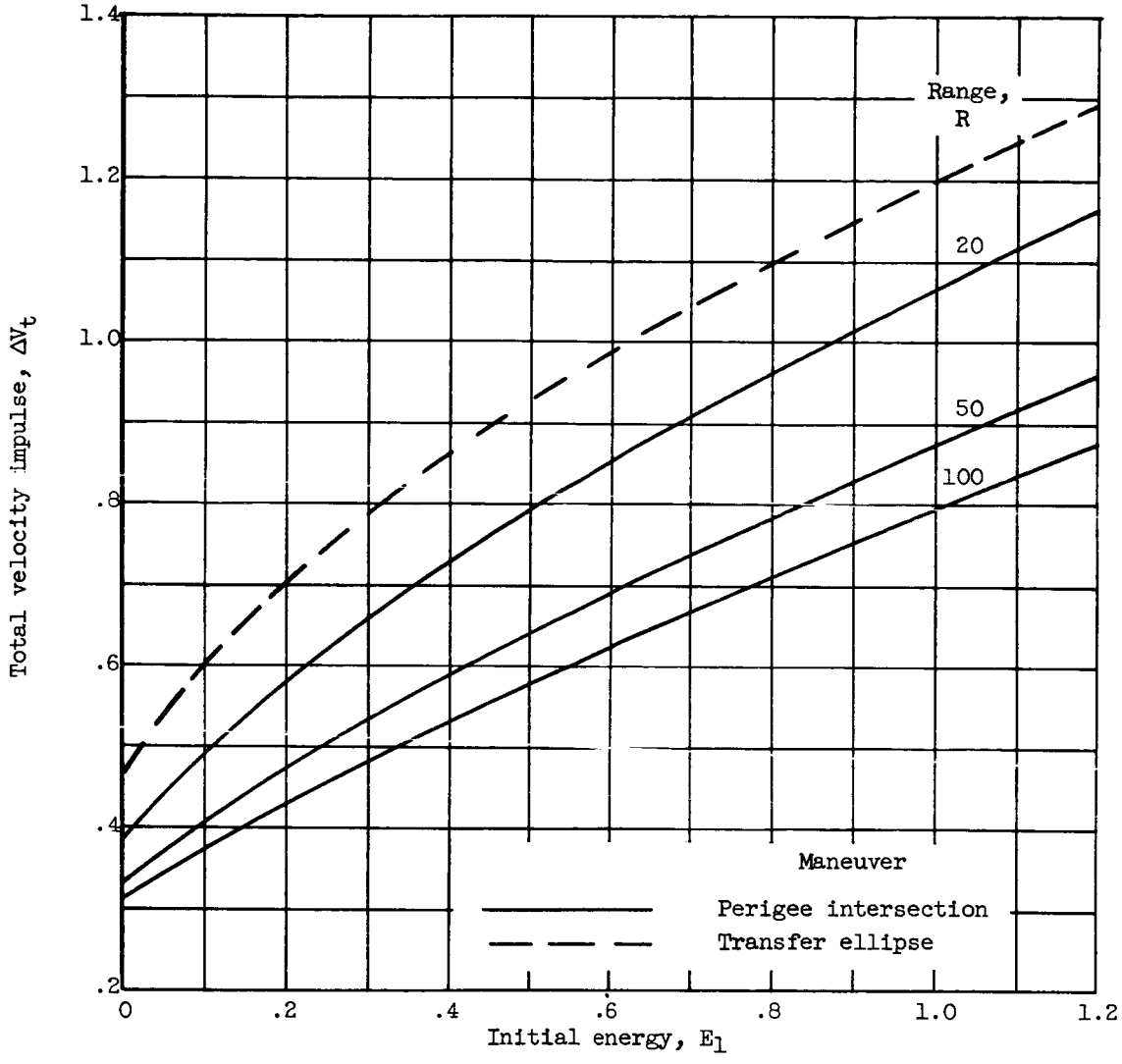

(c) Initial perigee, R_{p_1}, 10.

Figure 7. - Concluded. Required velocity impulse to transfer from approach trajectory to circular satellite orbit.

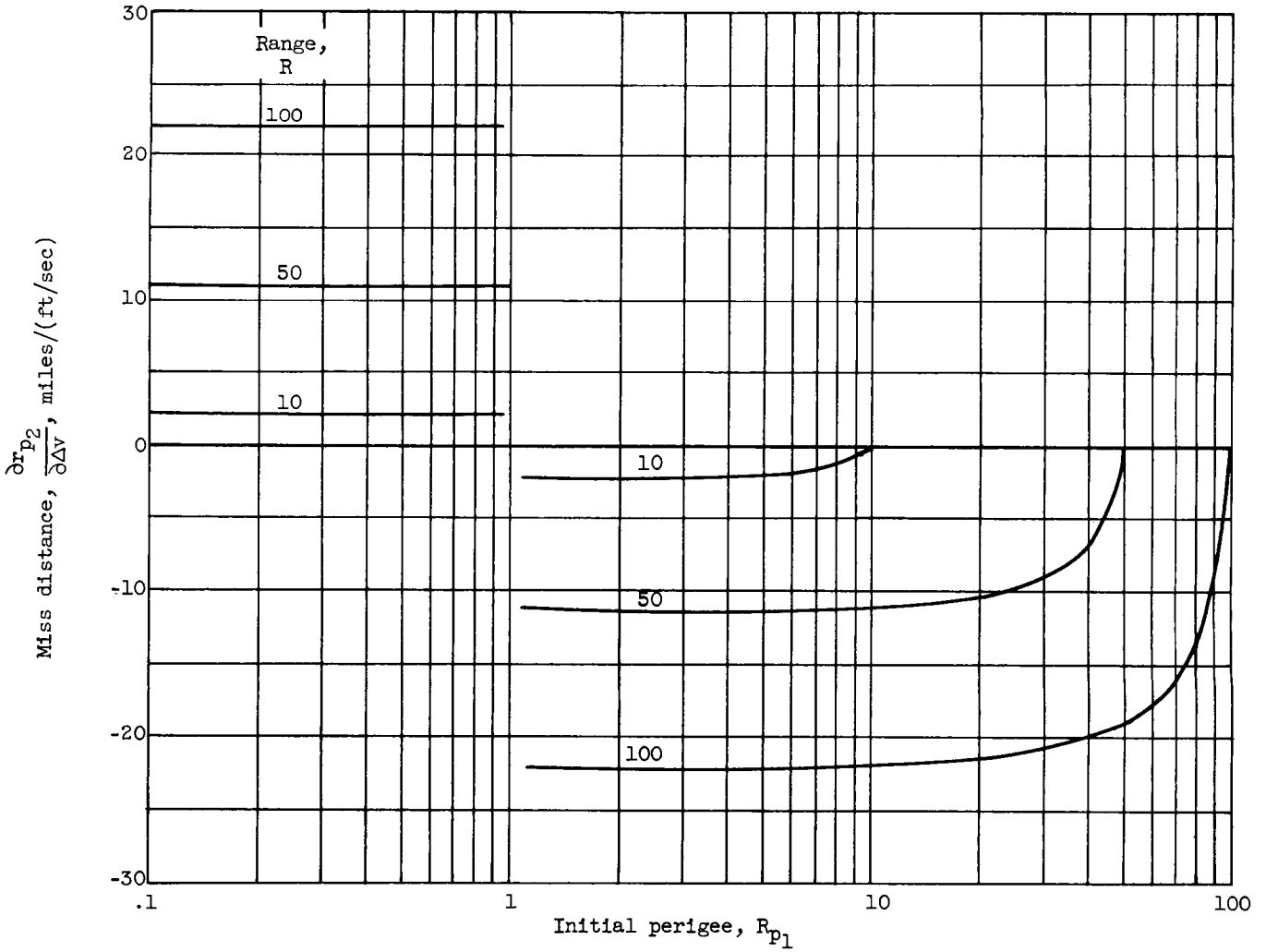

(a) Caused by impulse magnitude error.

Figure 8. - Miss distances. Earth approach. Initial energy, E_1, 0; target perigee, 40-mile altitude; r_{p_2}, 4040 miles.

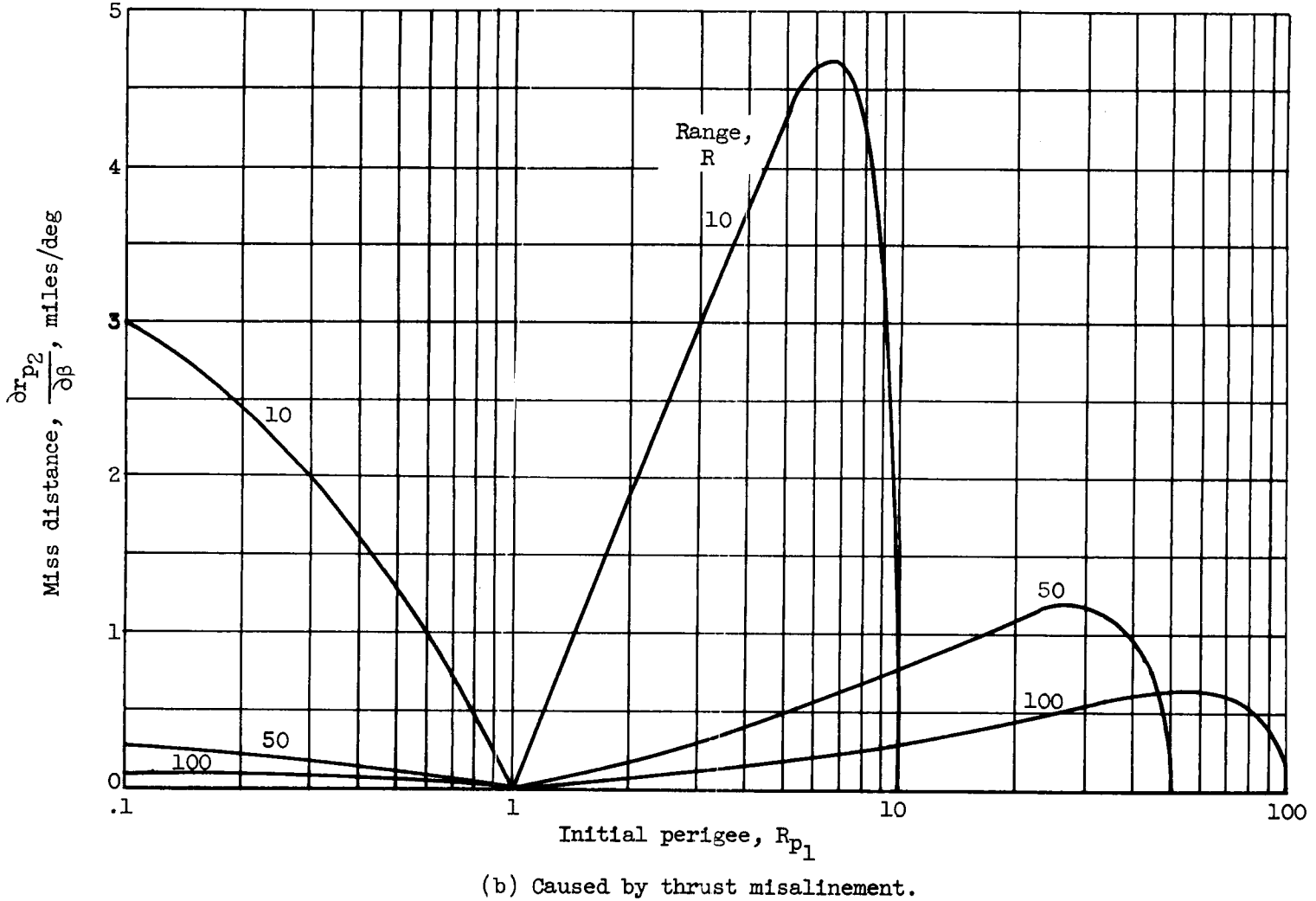

(b) Caused by thrust misalinement.

Figure 8. - Concluded. Miss distances. Earth approach. Initial energy, E_1, 0; target perigee, 40-mile altitude; r_{p_2}, 4040 miles.

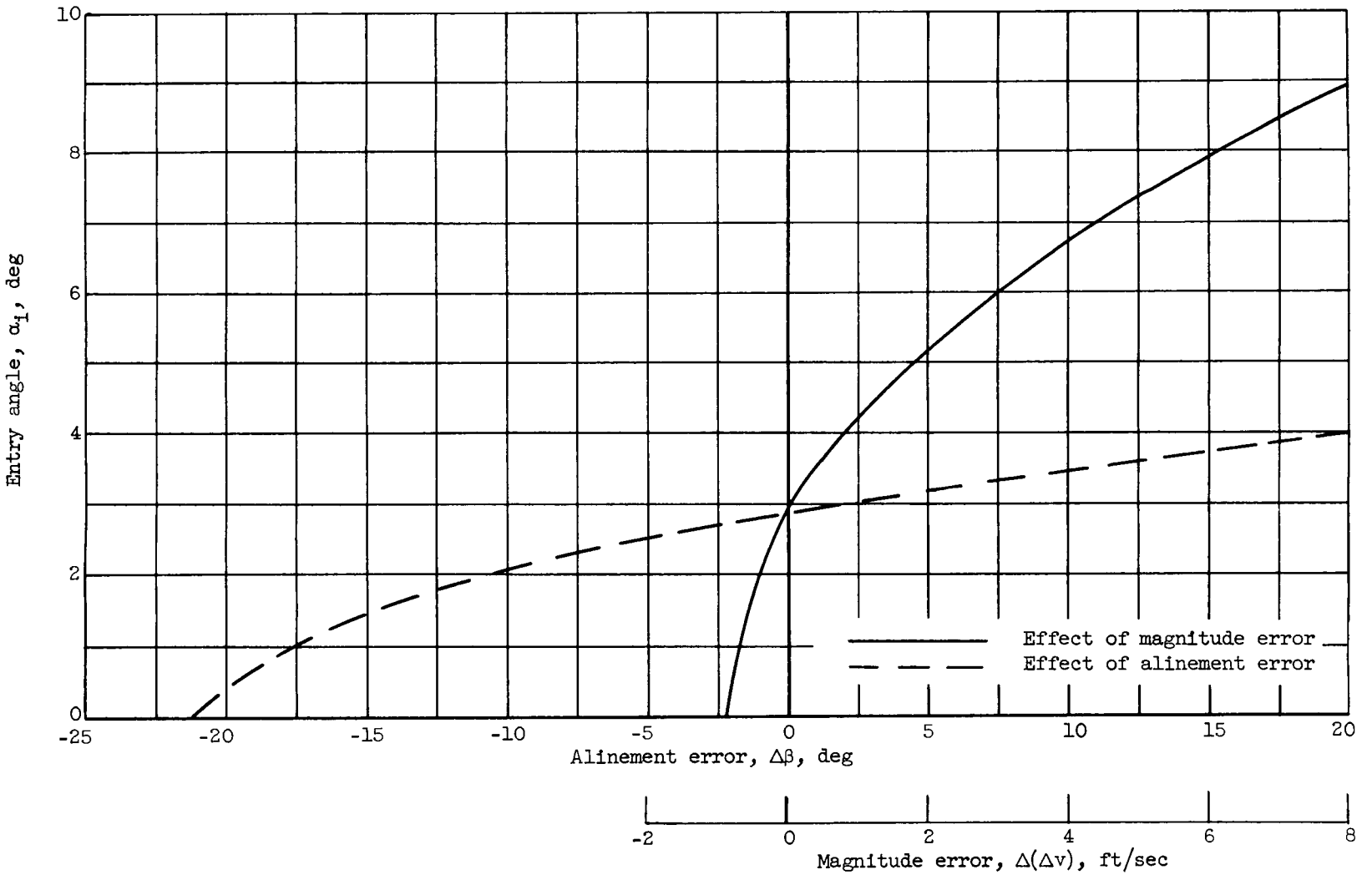

Figure 9. - Effect of thrust magnitude and alinement errors on atmospheric entry angle. Initial energy, E_1, 0; initial perigee, R_{p_1}, 5; range, R, 50.

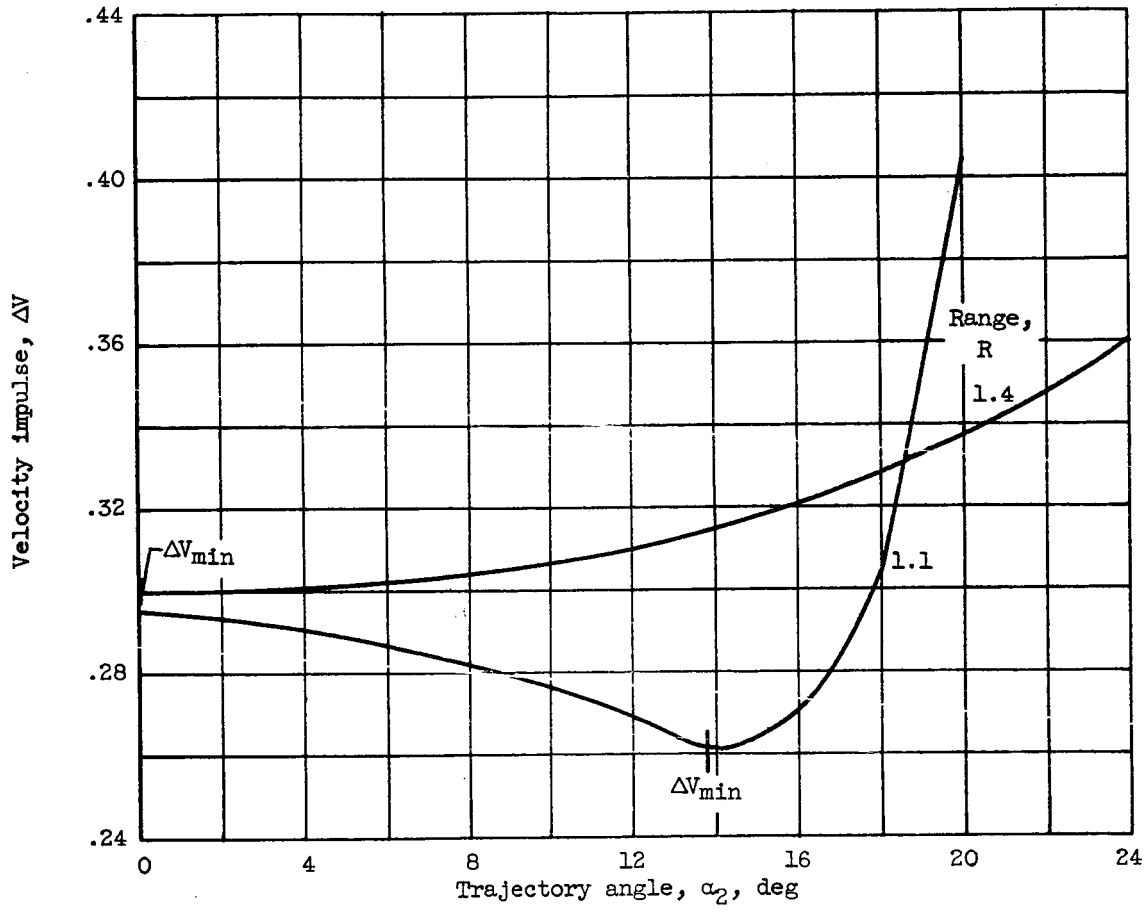

Figure 10. - Characteristic of optimum solution, special case. Initial energy, E_1, 0; $R = R_{p_1}$.